Morpholino Treatment Improved Muscle Function and Pathology in *Pitx1* Transgenic Mice

by Yi-Chien Lee

B.S. in Agronomy, June 2008, National Taiwan University

A Thesis submitted to

The Faculty of
Columbian College of Arts and Sciences
of The George Washington University
in partial fulfillment of the requirements
for the degree of Master of Science

May. 20th 2012

Thesis directed by

Yi-Wen Chen

Associate Professor of Integrative Systems Biology

Associate Professor of Pediatrics

Acknowledgements

This project is supported by NIH/NIAMS RO1 AR05 2027-03S1. I am sincerely and heartily grateful to my mentor, Dr. Yi-Wen Chen, for the support and guidance she showed me from the first day I joined the Chen lab throughout the whole project and my thesis writing. I am sure it would have not been possible without her help. Besides, I would like to thank Dr. Sachchida Nand Pandey who worked with me side by side during this morpholino project. His help was critical to the completion of this project. I am deeply grateful to my academic advisor Dr. Vanderhoek for carefully reviewing my thesis and for his support for my graduate studies.

It is a pleasure to thank all the members in the lab. Naoe always gave me the most professional advice both in science and daily life. San made my days in lab and outside of lab more inspiring and colorful. I would like to give my special thanks to JanNean for teaching me techniques for doing animal experiments and Dr. Yokota for teaching me intravenous injections in tail vein of mice. I also want to thank my friends and classmates in the biochemistry department. Learning with them is the most enjoyable thing.

Moreover, I would like to show my gratitude to my best friend Yi-Ting Tsai and the whole “U-Turn” group in Taiwan. Their timely support and warm encouragements always help me go through hard time.

Finally, I want to thank my family, my parents, my brother and Ting-Yu Chen. Even though they are far away from me, I always can strongly feel their love, care and support. Because of them, I have courage to face the difficulties and believe in myself, all the way forward towards my goal.

Abstract of Thesis

"Morpholino Treatment Improved Muscle Function and Pathology in *Pitx1* Transgenic Mice"

Paired-like homeodomain transcription factor 1 (*PITX1*) was proposed to be critically involved in facioscapulohumeral muscular dystrophy (FSHD). We generated a tet-repressible muscle-specific *Pitx1* transgenic mouse model in which expression of PITX1can be induced in skeletal muscle. In this study, we attempted to knock-down PITX1 expression using morpholino molecules designed to block translation of the *Pitx1* mRNA.

Three groups of the *Pitx1* transgenic mice (n=5) received weekly intravenous injections of phosphorodiamidate morpholino oligomers (PMO) (100mg/kg), octaguanidinium dendrimer-conjugated Morpholino (Vivo-morpholinos) (10mg/kg), or phosphate buffered saline (PBS) for six weeks. A group of control mice were used to provide baseline expression level of PITX1. The mice received the first injection of morpholinos when the oral doxycycline was discontinued to induce PITX1 expression, followed by weekly injections for six weeks. Four weeks after PITX1 induction, muscle function of the mice was evaluated by grip strength and rotarod testes. Triceps and quadriceps muscles were collected for H&E, immunohistochemistry and immunoblotting at the end of the 6th week.

Grip strength data showed that treatment with Vivo-morpholinos significantly ($p<0.05$) improved muscle function of the transgenic mice over-expressing *Pitx1* while the PMO treatment did not improve the muscle function. Immunohistochemistry and immunoblotting data showed that PITX1 protein expression in the triceps and quadriceps was reduced 2.7 ($p<0.05$) and 2.2 ($p=0.06$) folds respectively by the Vivo-morpholinos treatment but not the PMO treatment. The

pathology of the muscles of mice treated with Vivo-morpholinos was improved by showing significantly fewer angular atrophic myofibers ($p < 0.05$).

Pitx1 transgenic mice showed significant improvement in both muscle function and pathology after receiving Vivo-morpholinos injections, while the treatment of PMO didn't improve the phenotype. The results suggest that morpholinos can be a potential option for treatment development for FSHD.

Table of Content

Acknowledgements....ii

Abstract of Thesis....iii

Table of Content....v-vi

List of Figures....vii

List of Tables....viii

Abbreviation....ix

1. Introduction....1-10

1.1. Clinical presentations of Facioscapulohumeral muscular dystrophy....1

1.2. Genetics and molecular mechanisms of FSHD....1

1.3. The *Pitx1* transgenic mice model for FSHD....3

1.4. Morpholinos- a tool for gene correction and gene knockdown....5

1.5. The advantage of using PMO for antisense oligo therapy....6

1.6. Modify PMO to improve in vivo delivery....9

1.7. Aim of the study....10

2. Methods....11-17

2.1. Gene induction in the tet-repressible muscle-specific transgenic *Pitx1* mouse....11

2.2. Morpholino injections....12

2.3. Body, muscle and organ mass....13

2.4. Muscle function testing....14

2.5. Immunoblotting....15

2.6. Histology, immunohistochemistry, fiber diameter, and angular fibers calculation....15

2.7. Measurement of serum enzymes and other component....17

3. Results....18-35

3.1. Vivo-morpholinos against *Pitx1* reduced PITX1 protein in the *Pitx1* transgenic mice....18

3.2. Vivo-morpholinos treatments in *Pitx1* transgenic mice reduced PITX1 expression in nuclei....20

3.3. Grip strength is improved after Vivo-morpholinos treatments in the *Pitx1* transgenic mice....24

3.4. Muscle weight relative to body weight is improved in the *Pitx1* transgenic mice treated with Vivo-morpholinos 26
3.5. Vivo-morpholinos treatments improved pathology in the *Pitx1* transgenic mice..... 29
3.6. The fiber sizes of the mice treated with PBS, PMO and Vivo-morpholinos were not significantly different 29
3.7. Angular fibers were significantly fewer after Vivo-morpholinos treatments 33
3.8. PITX1 expression and percentage of angular fibers is highly correlated 34
3.9. Toxicity tests showed no obvious toxicity after Vivo-morpholinos treatments..... 35
4. Discussion 36-40
4.1. *In vivo* treatment for blocking protein translation 36
4.2. Side effects observation of PMO, PPMO and Vivo-morpholinos 37
5. References 41-47

List of Figures

Figure1. The subtelomeric region of chromosome 4q35 in normal individuals and in FSHD patients 2

Figure2. Skeletal muscles wasting in the *Pitx1* transgenic mice 4

Figure3. Morpholino oligo structure 5

Figure4. Conversion of riboneucleoside to Morpholino subunit 5

Figure5. Structure of Vivo-morpholinos 10

Figure6. tet-repressible muscle-specific *Pitx1* transgenic mice 11

Figure7. Time line for six I.V. injections and functional tests 13

Figure8. PITX1 knock down 18

Figure9. H&E and Immunohistochemistry staining 20

Figure10. Muscle functional tests by grip strength and rotarod 25

Figure11. Body weight and muscle weight observation 26

Figure12. Laminin staining and fiber size distribution 30

Figure13. Percentage of angular fibers 33

Figure14. Correlation of angular fibers and PITX1 expression level 34

Figure15. The levels of serum enzyme 35

List of Tables

Table1. Comparative properties of s-DNA, siRNA and PMO 8

Abbreviations

ALP: alkaline phosphatase

ALT: alanine transaminase

BUN: blood urea nitrogen

DMD: Duchenne Muscular Dystrophy

DT: double transgenic

DUX4: double homeobox protein 4

FRG1: FSHD region gene 1

FSHD: Facioscapulohumeral muscular dystrophy

Gas: gastrocnemius

GGT: r-glutamyl transferase

H&E: hematoxylin and eosin

IHC: immunohistochemistry

I.V.: intravenous injections

ORF: open reading frame

PBS: Phosphate Buffered Saline

PITX1: paired-like homeodomain transcription factor 1

PMO: phosphorodiamidate morpholino oligomers

PPMO: peptide-conjugated PMO

TA: tibialis anterior muscle

Vivo-morpholino: octaguanidinium dendrimer-conjugated morpholino

1. Introduction

1.1. Clinical presentations of Facioscapulohumeral muscular dystrophy

Facioscapulohumeral muscular dystrophy (FSHD) is a dominantly inherited dystrophy, with a prevalence of 1:20,000(Padberg 1982), which is the third common dystrophy. The onset of the disease occurs between ages of 7 to 20 (Tyler 1949). It starts with facial weakness and is followed by scapular fixator, humeral, truncal and lower-extremity weakness (Tawil 2008). Asymmetry of facial muscles, shoulder muscles and extremities is a common feature of FSHD (Carroll 1979). The clinical severity is different among patients. Some patients have mild symptoms but some become wheel-chair dependent. Extra-muscular symptoms of FSHD include retinal vascular disease and subclinical hearing loss in 60% and 75% of patients with FSHD respectively (Fitzsimons, Gurwin et al. 1987; Padberg, Brouwer et al. 1995).

Studies have shown that muscle pathology of FSHD is non-specific in general. However, 30% of patients have severe muscle inflammation which leads to misdiagnosis as polymyositis. Moreover, the presence of small angular fibers is commonly found in FSHD patients (Lin and Nonaka 1991). There are some other marked abnormal histopathological changes especially in patients with active clinical aggravation. For example, some patients had more degenerating and regenerating fibers. Few patients had inflammatory cell infiltration and connective tissue proliferation.

1.2. Genetics and molecular mechanisms of FSHD

Studies have shown that FSHD is associated with a deletion of *D4Z4* repeats from 11-1000 to 1-10 repeats in the chromosome 4q35 (van Deutekom, Wijmenga et al. 1993) (Figure 1). Several studies have proposed some mechanisms to explain how the deletion may activate gene

expression in this region (Gabellini, Green et al. 2002; Jiang, Yang et al. 2003; van Overveld, Lemmers et al. 2003; Masny, Bengtsson et al. 2004; Wegel and Shaw 2005; Zeng, de Greef et al. 2009). Most of the studies suggest that the loss of *D4Z4* repeats result in the epigenetic de-repression; such as hypomethlylation of one or more genes in or near the *D4Z4*. Those genes activated by the deletion of *D4Z4* repeats may contribute to the FSHD phenotype. Several potential candidate genes have been reported, including double homeobox protein 4 (*DUX4*), FSHD region gene 1 (*FRG1*), FSHD region gene 2 (*FRG2*), and adenine nucleotide translocase 1 (*ANT1*) (Gabellini, D'Antona et al. 2006; Dixit, Ansseau et al. 2007).

Figure 1. The subtelomeric region of chromosome 4q35 in normal individuals and in FSHD patients. Normal individuals have between 11 and 100 *D4Z4* repeats on both 4q35 alleles, while FSHD patients have fewer than 11 repeats in one 4q35 allele. Double homeobox protein 4 (*DUX4*), FSHD region gene 1 (*FRG1*), FSHD region gene 2 (*FRG2*), and adenine nucleotide translocase 1 (*ANT1*).

Each *D4Z4* repeat contains an open reading frame (ORF) for *DUX4*, which encodes for a double homeobox protein. *DUX4* is used to be considered as a junk DNA because it doesn't contain an intron, polyadenylated signal and it was not detected as expressed. However, a healthy individual without the *D4Z4* repeat doesn't cause FSHD, which suggests that the existence of *DUX4* is essential of developing FSHD (Gabriels J 1999). In 2007, our group proposed a model in which a functional *DUX4* RNA could be produced by the last *D4Z4* repeat

under the condition of a functional polyadenylation signal existing in an adjacent *pLAM* region (Dixit, Ansseau et al. 2007). The hypothesis was confirmed by study of Lemmers et al. (2010). They found that two specific polymorphisms in FSHD patients create the polyadenylation site for the distal unit of *D4Z4* contains, which may stabilize the transcript and produce a functional DUX4 protein which is toxic to muscle cells (Kowaljow, Marcowycz et al. 2007; Bosnakovski, Xu et al. 2008). Moreover, it has been shown that DUX4 protein is up-regulated in the muscles of patients with FSHD (Dixit, Ansseau et al. 2007). Therefore *DUX4* is believed to be the causative gene of FSHD.

Our previous study demonstrated that *DUX4* can activate a paired-like homeodomain transcription factor 1 (*PITX1*) (Dixit, Ansseau et al. 2007). FSHD patients showed up-regulation of *PITX1* expression. *PITX1* is critical in the development and postnatal function of the pituitary gland (Lamonerie, Tremblay et al. 1996; Tremblay, Lanctot et al. 1998). *Pitx1* also affects hindlimb development (Lanctot, Moreau et al. 1999; Logan and Tabin 1999; Szeto, Rodriguez-Esteban et al. 1999; Civas, Island et al. 2002; Kolfschoten, van Leeuwen et al. 2005; Liu and Lobie 2007; Calvisi, Ladu et al. 2011). The fetuses of *Pitx1* knockout mice showed remarkable structural changes in their hindlimbs (Marcil, Dumontier et al. 2003). Moreover, another study has shown that a mutation which abolishes the expression of *PITX1* resulted in asymmetric lower-limb malformations in humans (Gurnett, Alaee et al. 2008). Those studies suggest that *PITX1* may preferentially affect arms. *PITX1* may be one of the essential factors that are associated with the asymmetry of muscles in FSHD patients.

1.3. The *Pitx1* transgenic mice model for FSHD

Because of a lack of an ortholog of *DUX4* in the mouse genome (Bosnakovski, Daughters et al. 2009), it is not clear whether *DUX4* regulates expression of the same gene targets in the mice. This is supported by the fact a group of human germ line genes can only be regulated by *DUX4* in human myoblasts but not in mouse myoblasts. Due to the fact that *PITX1* is a direct transcriptional target of DUX4, and there is an ortholog in mice, we decided to study the involvement of *PITX1* in FSHD. First, we generated a tet-repressible muscle-specific *Pitx1* transgenic mouse model which over-expresses the *Pitx1* gene in skeletal muscles, and is controlled by oral administration of doxycycline. After *Pitx1* is over-expressed, mice showed muscle weakness, wasting (Figure. 2) and myofibers atrophy which are seen in FSHD patients. Muscle function tests, pathological and histochemical examinations suggested that the *Pitx1* transgenic mouse model is a promising animal model for FSHD (Pandey, Cabotage et al. 2012).

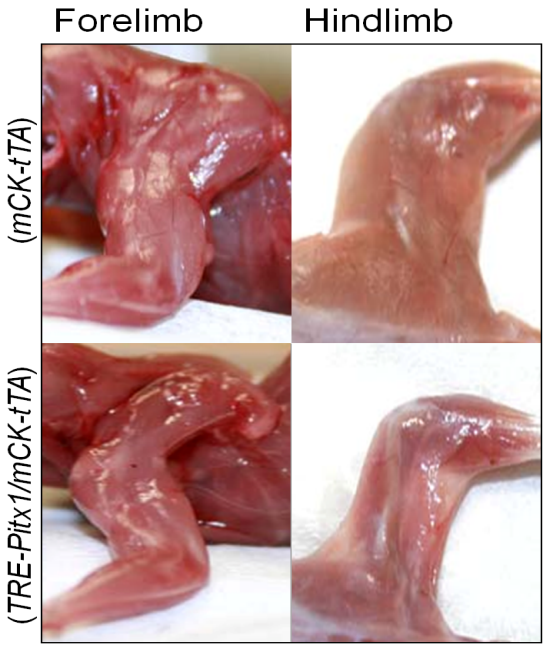

Figure 2. Skeletal muscles wasting in the *Pitx1* transgenic mice (*TRE-Pitx1/mCK-tTA*) vs. control mice (*mCK-tTA* or *TRE-Pitx1*) after 10 weeks of PITX1 over-expression

(Pandey, Cabotage et al. 2012).

1.4. Morpholinos- a tool for gene correction and gene knockdown

Morpholinos are called naked morpholinos or phosphorodiamidate morpholino oligomers (PMO). Two key structural features of PMO are the morpholino ring and a non-ionic backbone (Figure 3). The morpholino ring is synthesized from ribosides. The ribose ring is opened by oxidation and reclosed on ammonia (Figure 4). Then the product is reduced by $NaCNBH_3$ and becomes substituted morpholine (Moulton and Jiang 2009). One of the advantages of producing a morpholino ring from ribonucleosides is that this is a cheaper source than deoxyriboucleosides (Summerton 2005). The other key structure is the non-ionic backbone which protects the antisense oligos from enzymatic degradation. The phosphorodiamidate-linked backbone of PMO has high aqueous solubility as a result of better stacking of nucleobases (Kang, Chou et al. 1992).

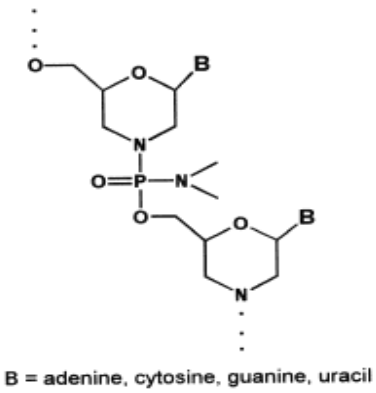

Figure 3. Morpholino oligo structure (Summerton J. 1997).

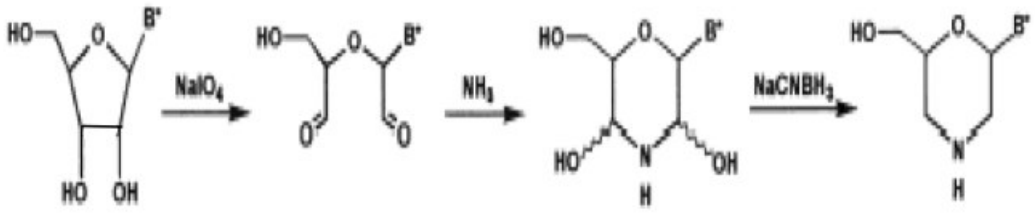

Figure 4. Conversion of riboneucleoside to morpholino subunit (Summerton J. 1997). The ribose ring is opened by oxidation, reclosed on ammonia, and then reduced to morpholino ring.

The mechanism of PMO is called steric blocking (Summerton 1999). By different mechanisms, morpholinos can block the translation of RNA, modify the splicing sites, and inhibit microRNA activity. To block the translation of RNA, PMO can be designed against the 5' UTR to the start codon region in order to prevent ribosomal subunits from binding to mRNA (Summerton and Weller 1997). Moreover, PMO can also modify splicing sites by binding to splice junctions, so spliceosomes can't recognize splice sites. Third, PMO can modulate miRNA processing and function by binding to the pre-miRNA or the mature miRNA respectively (Kloosterman, Lagendijk et al. 2007).

1.5. The advantage of using PMO for antisense oligo therapy.

Antisense oligos are mostly used for studying function and regulation of genes. Three classes of antisense oligos are widely used: RNase H dependent oligos such as S-DNA, RNA interference oligos such as siRNA, and steric block oligos such as PMO. There are advantages and disadvantages for each type of the oligos. Factors to be considered include (1) half-life (2) efficacy (3) specificity and off target effect.

PMO has the longest half-life. PMO replace the five-membered-ring sugar of DNA with a six-membered-morpholino rings. Negatively-charged phosphate linkages are replaced by the non-ionic phosphorodiamidate. These structural changes make PMO more stable (Hudziak, Barofsky et al. 1996). Moreover, PMO have a higher affinity to RNA than that of DNA binding RNA (Summerton 1999). PMO have non-charged backbones which allows for a simple and effective delivery by endocytosis. The replacement of one oxygen atom by a sulfur atom in the phosphate intersubunit linkages of the backbone of DNA results in the formation of S-DNA. S-

DNA has longer half-life than bare DNA and is less quickly degraded by nucleases. siRNA has a typical RNA structure. Therefore, it has a shorter half-life because of the degradation by RNases.

PMO have higher efficacy than S-DNA and siRNA. S-DNA is RNase H dependent and siRNA needs RISC complex as cofactors, while PMO work independently.

Sequence specificity is used to describe the ability of the antisense oligos to block the function of its target RNA without blocking functions of other RNAs in the cell. Minimum inhibitory length is one of the key values that affect sequence specificity (Summerton 2007). The minimum inhibitory length shows the shortest length of an antisense agent which must bind to the RNA target in order to inhibit the expression. PMO have been shown to require minimum target sequences of 14 bases, while S-DNA and siRNA require only 8 and 9 bases respectively. Therefore, PMO have better sequence specificity.

Off target effects are often used to describe effects which do not depend on Watson/Crick pairing. S-DNA has sulfur atoms on the backbones which may cause S-DNA bind to other proteins. It is believed that PMO are free from off target effects for the following reasons: PMO do not have charged backbones, so they have fewer interactions with proteins. PMO don't stimulate innate immune responses even when they contain CG sequences. Moreover, PMO containing tetraG don't interact with other proteins (Summerton 2007). On the other hand, it has been reported that S-DNA binds to laminin, bFGF, protein kinase C etc. (Stein 1984). S-DNA containing CG sequences that are not methylated at the 5 position of the cytosines will stimulate the body's innate immune system (Krieg, Yi et al. 1995). Moreover, S-DNA in the tetraG complexes has high affinity for heparin-binding protein such as Sp1 transcription factor. It has been shown that S-DNA activates Sp1 transcription factor which results in other effects

(Yaswen, Stampfer et al. 1993). For siRNA, it has been found that siRNA may stimulate interferon response (Sledz, Holko et al. 2003) and induce methylation of DNA and histone H3 (Kawasaki and Taira 2004).

In summary, PMO have high stability, high efficacy, and high specificity and they are free from off target effects. As a result, PMO appear to be the best reagent for gene knock down experiments.

Table1. Comparative properties of s-DNA, siRNA and PMO.

	RNase H-dependent oligos: Phosphorothioate-linked DNA (S-DNA)	RNA interference oligos: siRNA	Steric block oligos: PMO
Efficacy	Need Cofactor: RNase H	Need Cofactor: RISC complex	No need for cofactor
Structure advantage	1. be degraded less quickly by nuclease 2. similar to DNA so RNase H will cleave RNA strand of S-DNA/RNA duplex	1. typical RNA structure→ less off target effect	1. six-member morpholino rings 2. highly unnatural non-ionic phosphorodiamidate inter-subunit linkage→ not interact with proteins, simple and easy delivery 3. exceptional base stacking→ high solubility
Structure disadvantage	1. sulfurs cause S-DNA bind to proteins→ off target effect		
Affinity to RNA	Low	Middle	High
Efficacy	Need Cofactor: RNase H	Need Cofactor: RISC complex	No need for cofactor
Minimum inhibitory length	8	9	14
Off target effect	1. activation of complement cascade 2. non-methylated CG sequences→ innate immune system 3. tetraG→ high affinity for heparin-binding proteins, activate Sp1 TF 4. bind to other proteins	1. RNA/RNA→Interferon stimulation 2. induce DNA and H3 methylation in human cells	1. no protein interaction 2. no activation of complement cascade 3. no stimulation of innate immune responses 4. no binding to macromolecular component of serum and blood 5. no activation of interferon responses 6. not degraded in biological system

1.6. Modify PMO to improve *in vivo* delivery.

The non-charged backbone of PMO causes difficulty in delivery of PMO molecules into the target cells. To solve the problem, several modifications have been developed and tested for better delivery. For instance, arginine-rich cell-penetrating peptide conjugated PMO called PPMO is a technology developed to allow enough of endocytosed oligos to escape from endosomes to have biological activities. Studies have shown that the guanidinium moiety of ariginines enhances the uptake of conjugated materials into endosomes (Wender, Mitchell et al. 2000). Moreover, the cell penetrating peptides also enhance endosomal escape (Abes, Moulton et al. 2008). The positively charged guanidinium moieties may attract phosphate groups on the membrane and also form hydrogen bonds with oxygen of phosphate groups (Rothbard, Jessop et al. 2004). These interactions may disturb the endosomal membrane and make it more permeable.

In this study, we used commercialized octaguanidinium dendrimer-conjugated morpholino oligomers from Gene Tools, LLC (Philomath, OR, USA) called Vivo-morpholinos. Vivo-morpholinos comprises a dendritic structure assembled around a triazine core which uses to position eight guanidinium head groups (Morcos, Li et al. 2008) (Figure 5). Just like PPMO, the guanidinium head groups may interact with phosphates of phospholipids both by electrostatic attraction and hydrogen bonds.

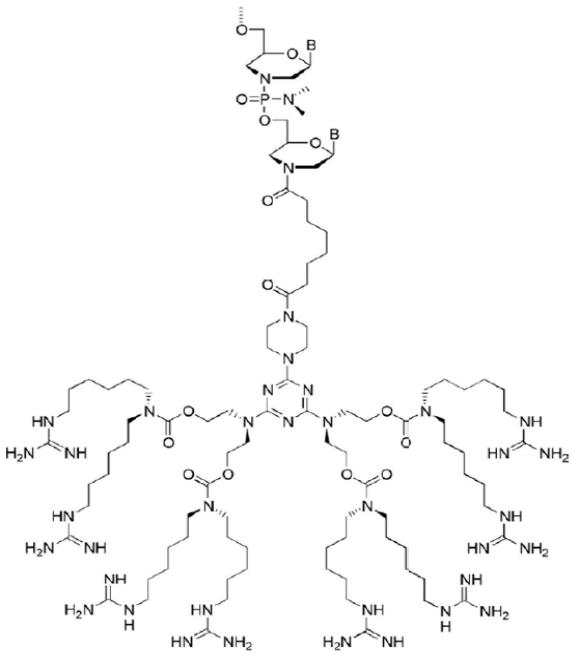

Figure 5. **Structure of Vivo-morpholinos** (Paul A. 2008). Two 3' end bases from a morpholino oligomer linked to dendritic octaguanidium head groups.

1.7. Aim of the study

In this study, we hypothesized that Vivo-morpholino but not PMO will knock-down the expression of PITX1 in muscles of the *Pitx1* transgenic mice. As a consequence, the mice treated with Vivo-morpholino will show improvement of muscle function and pathology. The findings will help us evaluate the strategy as a potential therapeutic mean of FSHD. It can also be applied to other genetic diseases in which the causative genes/proteins need to be suppressed.

2. Methods

2.1. Gene induction in the tet-repressible muscle-specific transgenic *Pitx1* mouse

All animal procedures were approved by the IACUC committee at the Children's National Medical Center in Washington, DC. Two transgenic mouse lines (*TRE-Pitx1* and *mCK-tTA*) were cross-bred in order to generate the tet-repressible muscle-specific *Pitx1* transgenic mice (*TRE-Pitx1/mCK-tTA*). The *TRE-Pitx1* line carries a construct containing the *Pitx1* gene, driven by a tretracycline response element (*TRE*). The *mCK-tTA* line carries a construct containing the *tTA* gene, driven by a muscle specific creatine kinase promoter (*mCK*) as previously reported (Ghersa, Gobert et al. 1998) (Figure 6).

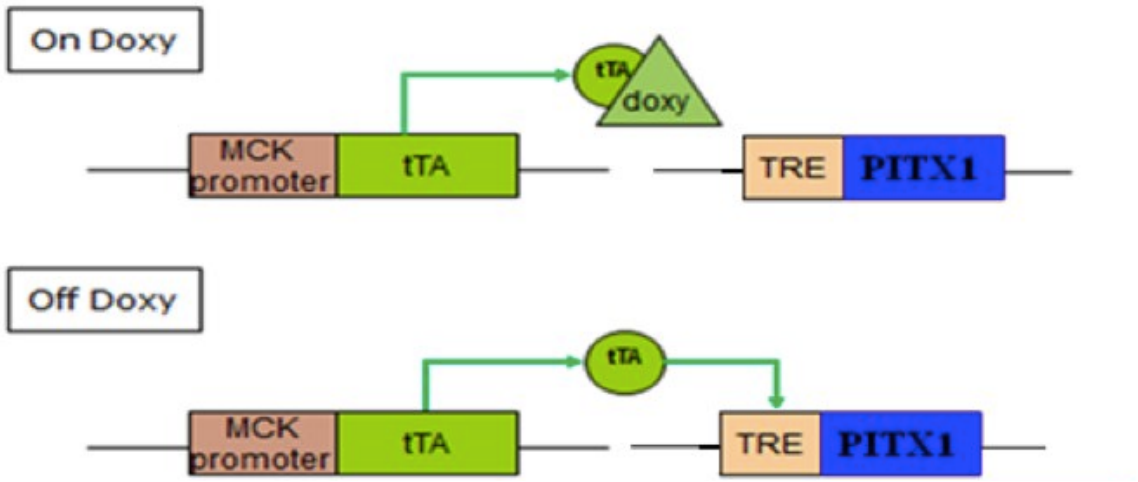

Figure 6. tet-repressible muscle-specific *Pitx1* transgenic mice (*TRE-Pitx1/mCK-tTA*). The *tTA* mice express tTA (tetracycline-controlled transactivator protein) under the control of the creatine kinase promoter (*mCK*), which is muscle-specific. The *TRE-Pitx1* mice carry *Pitx1* gene controlled by the *TRE* (tetracycline response element). *TRE-Pitx1* mice were cross-bred with *mCK-tTA* mice to generate double transgenic mice. By adding doxycycline in drinking water, doxycycline binds to the tTA protein, preventing it from binding to the *tetOff* promoter, hence prevent PITX1 expression.

The female mice received drinking water with doxycycline (200 μ g/ml with 5.0 % sucrose) in order to suppress the *Pitx1* transgene expression in the pups *in utero*. Under these conditions, the *TRE-Pitx1/mCK-tTA* double transgenic (DT) mice were born at the expected Mendelian ratio. The pups continued to receive doxycycline through the mother's milk. After weaning, all pups were maintained on water treated with doxycycline until they were entered into an experimental regime. For all experiments, littermates carrying a single transgene (*Pitx1* or *tTA*) were used as controls.

To identify mice carrying one or two of the transgenes (*Pitx1* and *tTA*), we collected a small piece of tail tip and isolated DNA for genotyping. The following primers were used for polymerase chain reaction (PCR) amplification. For *Pitx1*: forward 5'-TGG AGG CCA CGT TCC AAA G-3' and reverse 5'- GTT CTT GAA CCA GAC CCG CAC-3'; for *tTA*: forward 5'-ACAGCGCATTAGAGCTGCTT-3' and reverse 5'-CCCCTTCTAAAGGGCAAAAG -3'.

2.2. Morpholino injection

The oligonucleotide sequence 5'- TCATGCCTCCCTTGAAGGCGTCCAT -3', against the start codon of *Pitx1* was synthesized as morpholinos by Gene Tools, LLC (Philomath, OR, USA). PMO and Vivo-morpholinos were used in this study. Vivo-morpholinos were made by conjugation of an unmodified morpholinos (PMO) with a triazine core scaffold featuring eight guanidinium head groups. Both PMO and Vivo-morpholinos were dissolved in PBS and delivered directly. Intravenous injections were applied weekly for six weeks to 12 *Pitx1* transgenic mice and five control littermate mice (Figure 7). PMO and Vivo-morpholinos doses were 100mg PMO per kilo-gram of body mass and 10mg Vivo-morpholinos per kilo-gram of body mass respectively. PMO dissolved in 100 µl PBS were injected into three *Pitx1* transgenic

mice and Vivo-morpholinos were injected into five *Pitx1* transgenic mice. Four *Pitx1* transgenic mice, one *tTA* mouse, and four *Pitx1* mice were injected 100µl PBS as control.

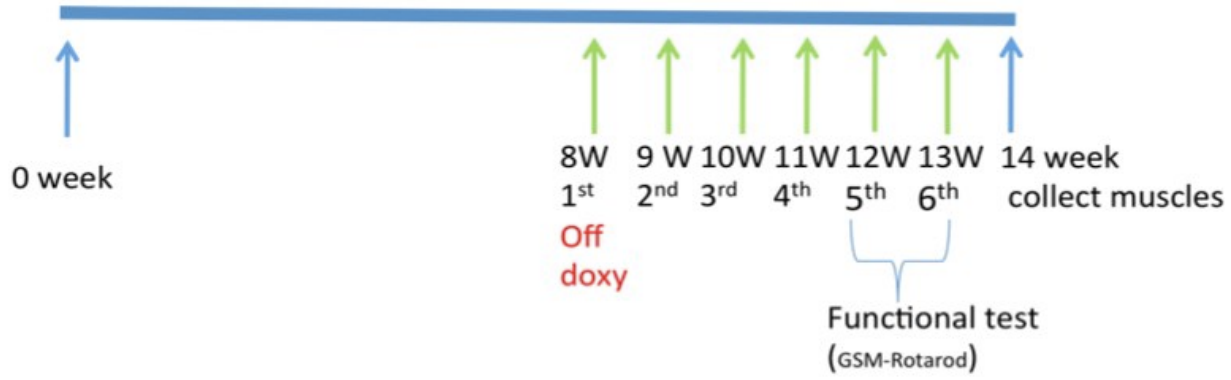

Figure 7. Time line for six I.V. injections and functional tests. Doxycycline water was removed after mice reached eight weeks old and the first intravenous (I.V.) injection was applied. Mice received I.V. injections once a week for six weeks. After the fifth and sixth injection, grip strength and rotarod were applied respectively. Mice were sacrificed and collected at 14 weeks old.

2.3. Body, muscle and organ mass

The body weight of 12 *Pitx1* transgenic (*TRE-Pitx1/mCK-tTA*) male mice and five control littermate male mice (*TRE-Pitx1*or *mCK-tTA*) were measured every two days, starting from the date that doxycycline was first removed from their water. After being off doxycycline for six weeks, the mice were euthanized. Masseter, soleus, tibialis anterior, quadriceps, gastrocnemius, deltoid, triceps, biceps, diaphragm, liver, heart, kidney, spleen and brain from 12 *Pitx1* transgenic mice and five control mice were dissected and immediately weighed. The data were expressed as the mean ± s.e. Significant differences between the induced *Pitx1* transgenic mice and the controls were tested by one-tailed T test. The significance cutoff was $p<0.05$.

2.4. Muscle function testing

The grip strength test (Grip Strength Meter, Columbus Instruments, Columbus, OH, USA) and the rotarod test (Columbus Instruments, Columbus, OH, USA) were performed on 12 *Pitx1* transgenic mice and five control littermates. The mice were eight weeks old when the doxycycline was removed from their drinking water and mice receive intravenous injections weekly. The functional tests were performed after giving fifth I.V. injections (Figure 7).

The Grip Strength Meter (GSM) consists of two steel grids connected to force meters. The forelimb grid is horizontal and the hind limb grid is angled. Grip strength is tested by holding the mouse over the grid until the mouse can grip the steel bars. Then the mouse is pulled away from the force meter until it releases the grid. The meter records the maximum force that was applied. The mice were acclimated for twenty seconds to the GSM for two consecutive days prior to data collection. They were then tested once a day for five consecutive days; five measurements were recorded for each test. The largest measurements from each of the five tests were averaged and normalized to body weight (g).

For the rotarod test, the mice were acclimated to the rotarod apparatus for two consecutive days prior to data collection. During acclimation the mice were placed on the rotarod twice a day for two minutes, at a speed of five rotations per minute. If the mice fell off the cylinder before the two minutes were up, they were placed back on the cylinder. After acclimations, the mice were then tested twice a day for three consecutive days. During each test, the cylinder was set at a speed of 10 rotations per minute for one minute. If the mice fell off the cylinder before the minute was up, they were placed back on the cylinder. After one minute the speed accelerated at a rate of 1.2rotations per second until it reached 40 rotations per minute. Starting at the beginning of the acceleration phase, the length of time (in seconds) that each

mouse could stay on the cylinder before falling off was recorded. The maximal running time is 180 seconds. The final score was determined by averaging the recorded time from all six trials.

2.5. Immunoblotting

Muscle sections were digested with a hand sonicator for 10 seconds at room temperature in lysis buffer (50 mM Tris-HCL, pH 7.5, 150 mM NaCl, 0.5% sodium deoxycholate, 1% NP40, 0.1% SDS, and protease inhibitor). Protein concentration was determined by *DC*^{TM} protein assay (Bio-Rad, Hercules, CA, USA), and 50 µg of protein was loaded onto 4-12% Bis-Tris NuPage Mini Gels (Invitrogen, Carlsbad, CA, USA) then transferred to Hybond nitrocellulose membranes (Amersham Biosciences, Little Chalfont, Buckinghamshire, UK). After blocking, the membrane was incubated with rabbit polyclonal anti-PITX1 antibody (1:2,500) (Dixit, Ansseau et al. 2007) followed by secondary antibodies conjugated with HRP (Amersham Biosciences**,** Little Chalfont, Buckinghamshire, UK). Chemiluminescent substrate (Pierce, Rockford, IL, USA) was used to visualize the target proteins on blue light autorad film (BioExpress, Kaysville, UT, USA). Detection of loading control Vinculin (abcam, Cambridge, MA, USA) was similarly performed with 1:20000 dilution of the mouse monoclonal primary antibody. Band density of the target protein was measured using a GS 800 Calibrated Densitometer (Bio-Rad, Hercules, CA, USA) then normalized to the density of Vinculin.

2.6. Histology, immunohistochemistry, fiber diameter, and angular fibers calculation

Eight week-old mice were off oral doxycycline and receiving I.V. injections for six weeks before muscle collection. Immediately after dissection, the whole muscles were snap-frozen in isopentane cooled with liquid nitrogen, then stored at -80 °C until sectioning. A Leica CM 1900 cryostat (Walldorf, Baden-Wurttenberg, Germany) was used to prepare cryosections for all the following histological analyses. H&E staining was conducted using 8 µm sections.

Five random non-overlapping fields of the tissue section were imaged using Nikon Eclipse E800 microscope (Nikon, Chiyoda-ku, Tokyo, Japan), RT slider camera (Diagnostic Instrument, Sterling Height, MI, USA) and SPOT advanced software.

For immunohistochemistry, 4 µm muscle sections were fixed in cold acetone for 10 min, and then incubated with primary antibody at 4 °C overnight. The primary antibodies used for PITX1 is rabbit polyclonal anti-PITX1 (1:500) (Dixit et al., 2007). The ABC kit (Vectors Lab, Burlingame, CA, USA) was then used to detect the primary antibody bound target proteins. The sections were stained with nuclear dye Hoechst 33258 (1:2500 dilution) to visualize nuclei. The muscle sections were imaged using Nikon Eclipse E800 microscope, RT slider camera and SPOT advanced software.

To measure myofiber diameter, 4 µm cryosections were prepared. The sections were fixed using cold acetone, blocked using 10% horse serum, and then incubated with rabbit anti-laminin antibody (Sigma, Saint Louis, MO, USA) at a dilution of 1:400. After the sections were washed three times with PBS, we applied Cy2 donkey anti-rabbit antibody (Jackson Immuno Research, West Grove, PA, USA) at a dilution of 1:500. The images of 5 random fields were processed using Image J software (NIH) and the minimal Feret's diameter was measured. To obtain the actual micron size we set a scale using a microscope scale (Graticules) where 1 pixel = 5.40 µM. The fibers were first ranked based on their size than the rank number was divided by the total number of fibers to obtain a value between 0 to1. This number (Y-axis) is then plotted against the fiber diameter (X-axis). The Kolmogorov-Smirnov test was used to determine the significance of the difference in fiber size distribution (www.physics.csbsju.edu/stats/KS-test.n.plot_form.html).

To calculate angular fibers, five random non-overlapping fields of H&E staining of quadriceps sections were imaged using Nikon Eclipse E800 microscope (Nikon, Chiyoda-ku, Tokyo, Japan), RT slider camera (Diagnostic Instrument, Sterling Height, MI, USA) and SPOT advanced software. Angular fibers and total fibers of each image were calculated using Image J software (NIH) in a masked manner to minimize bias.

2.7. Measurement of serum enzymes and other component

Blood samples were collected immediately after the mice were euthanized. Serum was separated and stored at -80°C. The levels of alkaline phosphatase (ALP) (U/dL), alanine transaminase (ALT) (U/dL), blood urea nitrogen (BUN) (mg/dL), creatine kinase (kU/L), creatine (mg/dL), r-glutamyl transferase (GGT) (U/L), and total bilirubin (mg/L) were determined by Comparative Clinical Pathology Services, LLC (Columbia, Mo).

3. Results

3.1. Vivo-morpholinos against *Pitx1* reduced PITX1 protein in the *Pitx1* transgenic mice.

To determine whether the over-expressed PITX1 protein level was knock-downed by the PMO and Vivo-morpholinos, immunoblotting was conducted using proteins from the triceps and quadriceps. *Pitx1* expression of the mice treated with Vivo-morpholinos was 2.97 fold lower ($p<0.05$) than the *Pitx1* transgenic mice treated with PBS, while PMO treatment did not cause difference (Figure 8A1). *Pitx1* expression in quadriceps of the mice treated with Vivo-morpholinos was 2.11 fold lower ($p=0.06$) than *Pitx1* transgenic mice treated with PBS (Figure 8B1). Again, PMO treatment did not affect PITX1 expression.

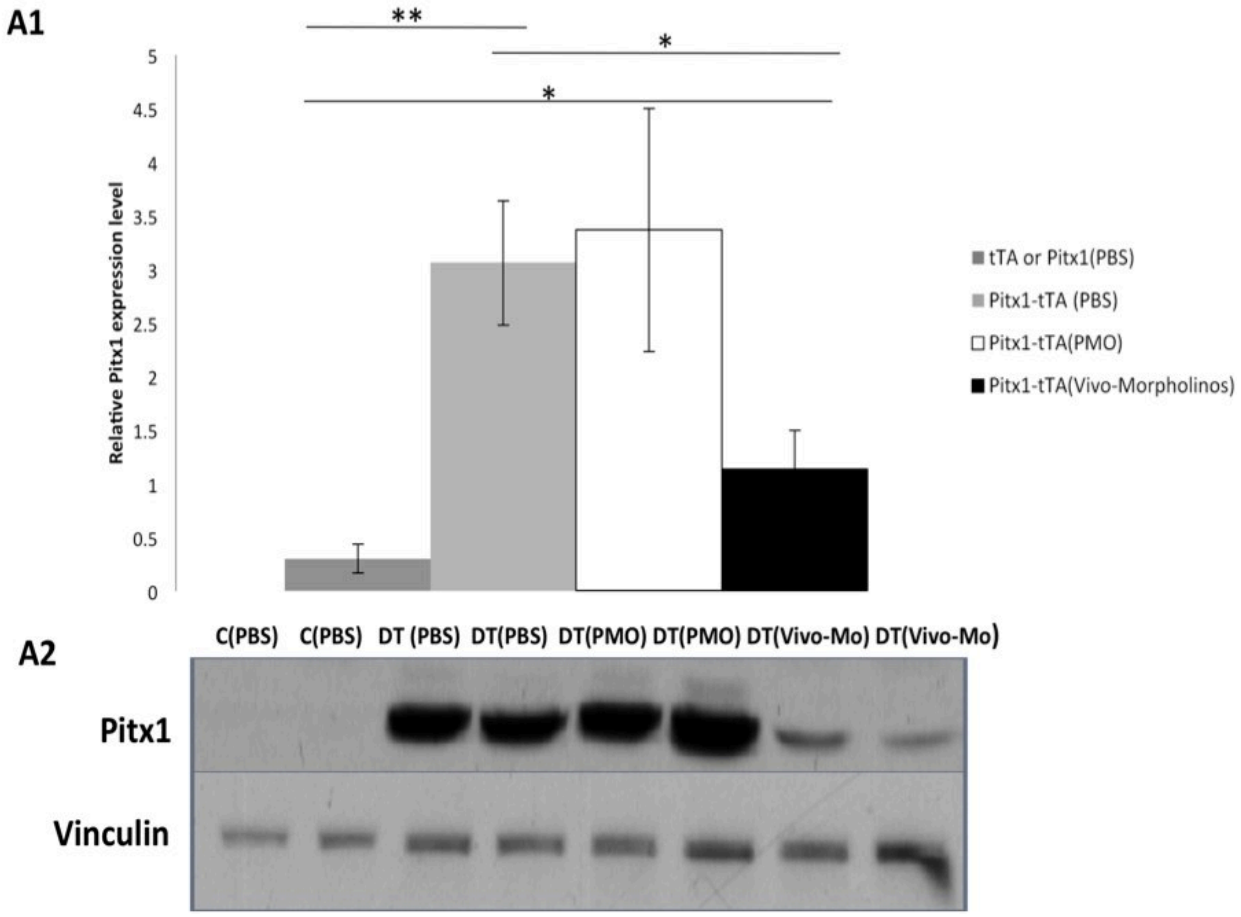

Figure 8A. (1) The expression levels of averaged PITX1protein in triceps of *Pitx1* transgenic mice (*TRE-Pitx1/mCK-tTA*) and control mice (*mCK-tTA* and *TRE-Pitx1*) after different treatments of six I.V. injections. One asterisk indicates significant differences with $p < 0.05$, and two asterisks indicate $p < 0.01$. (2) Immunoblotting of PITX1 and Vinculin. Vinculin is the internal control. C represents control mice, and DT represents *Pitx1* transgenic mice. Treatments received are indicated in the parentheses. There are duplicates for each group.

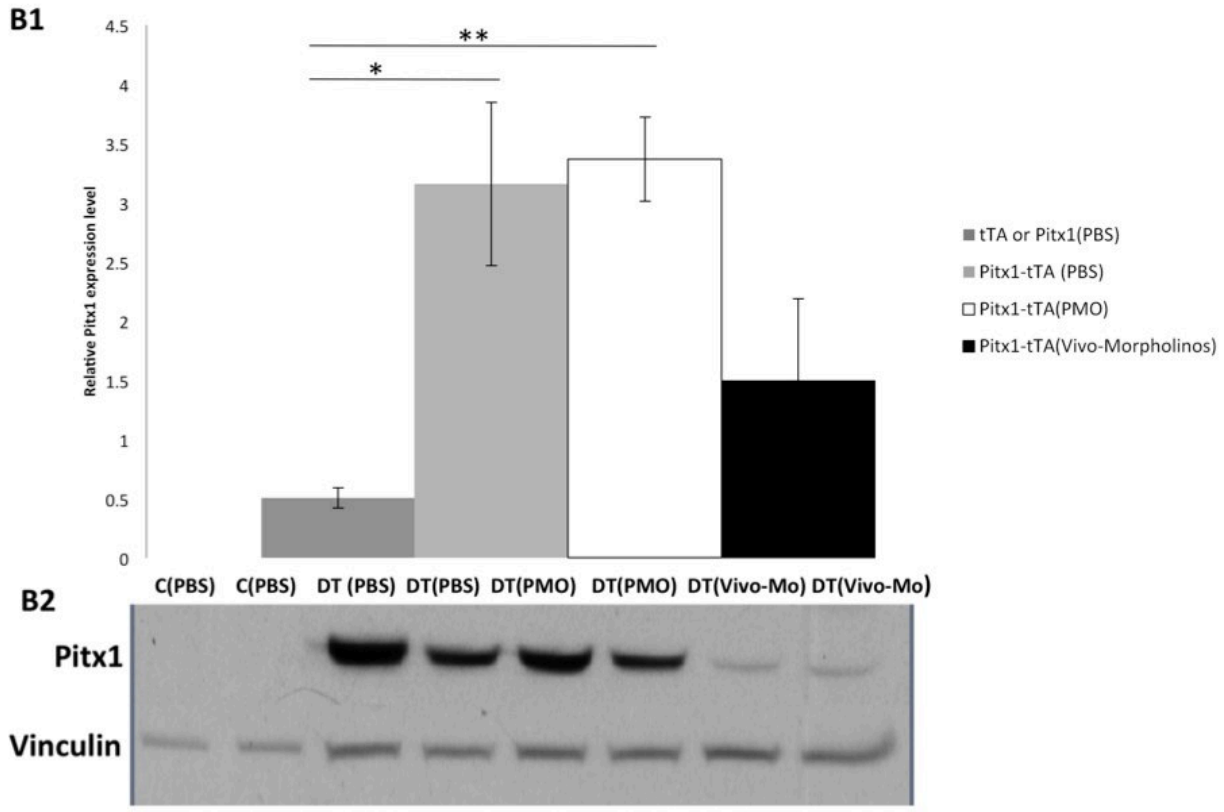

Figure 8B. (1) The expression levels of averaged PITX1protein in quadriceps of the *Pitx1* transgenic mice (*TRE-Pitx1/mCK-tTA*) and control mice (*mCK-tTA* or*TRE-Pitx1*) after different treatments of six I.V. injections. One asterisk indicates significant differences with $p < 0.05$, and two asterisks indicate $p < 0.01$. (2) Immunoblotting of PITX1 and Vinculin. Vinculin is the internal control. C represents control mice, and DT represents *Pitx1* transgenic mice. Treatments received are indicated in the parentheses. There are duplicates for each group.

3.2. Vivo-morpholinos treatments in *Pitx1* transgenic mice reduced PITX1 expression in nuclei.

To examine the PITX1 knock down in myofibers, triceps and quadriceps were sectioned and stained with PITX1 antibody. Control mouse showed no detectable PITX1 expression in nuclei (Figure 9A). A large amount of PITX1 expression in nuclei was observed in muscle sections of the *Pitx1* transgenic mice treated with PBS (Figure 9B). Mice treated with PMO had a large number of PITX1 positive nuclei (Figure 9C). Mice treated with Vivo-morpholinos showed less PITX1 positive nuclei (Figure 9D). The results of immunoblotting and immunohistochemistry indicated that the PITX1 expression of the mice treated with the Vivo-morpholinos was suppressed by treatment, while the PMO did not affect the PITX1 expression.

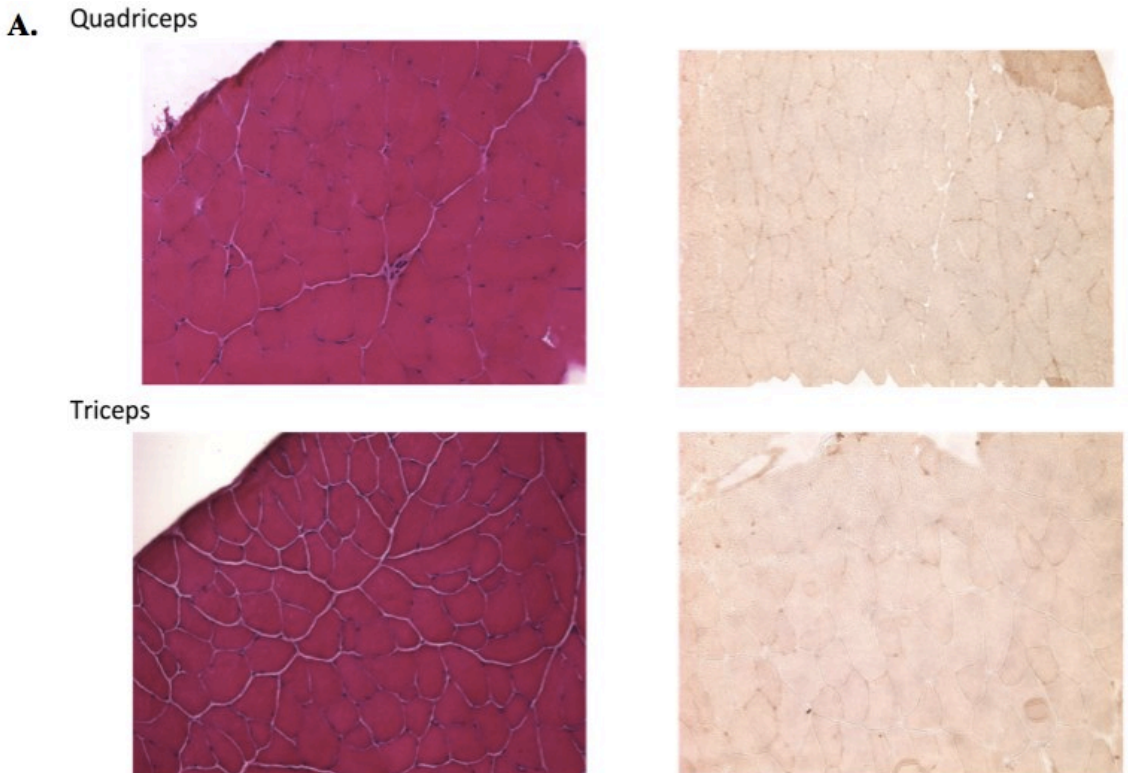

Figure 9A. Hematoxylin and eosin (H&E) staining (left) of control mouse showed healthy muscle fibers without angular fibers and fibers with central nuclei. Immunohistochemistry (IHC) (right) showed no PITX1 positive nuclei.

B.

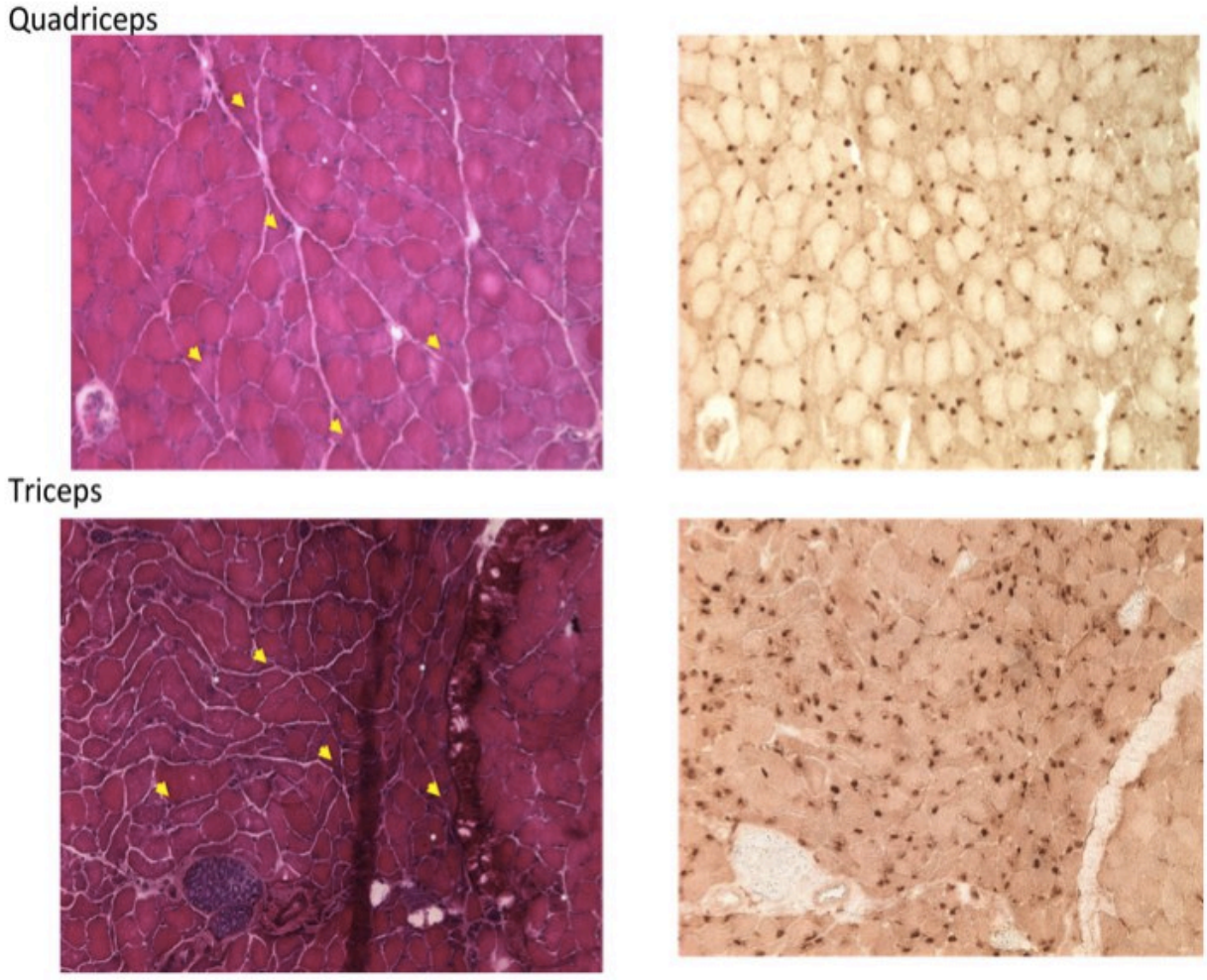

(B) H&E (left) staining of *Pitx1* transgenic (*TRE-Pitx1/mCK-tTA*) mouse treated with PBS showed massive amount of angular fibers and fibers with central nuclei. Immunohistochemistry (right) stains PITX1 positive nuclei. Arrows indicate angular atrophic myofibers and asterisks indicate myofibers with central nuclei.

C.

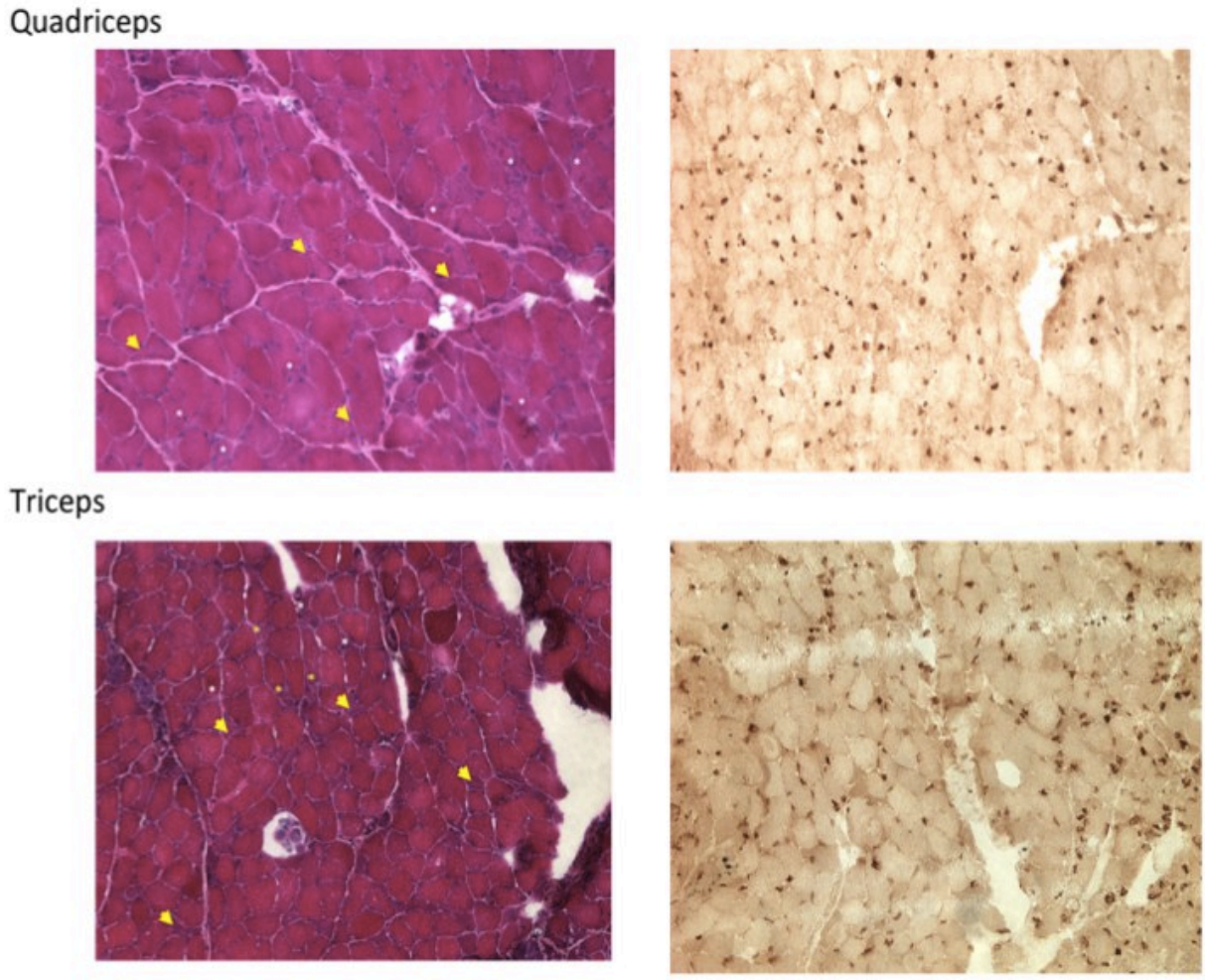

(C) H&E (left) staining of *Pitx1* transgenic (*TRE-Pitx1/mCK-tTA*) mouse treated with PMO didn't show obvious pathological improvement. H&E staining has angular fibers and fibers with central nuclei. Especially, in triceps, there are high number of degenerating and regenerating fibers (indicated by yellow asterisks). Immunohistochemistry (right) stains PITX1 positive nuclei. The amount of PITX1positive nuclei is similar with the *Pitx1* transgenic (*TRE-Pitx1/mCK-tTA*) mouse treated with PBS.

D.

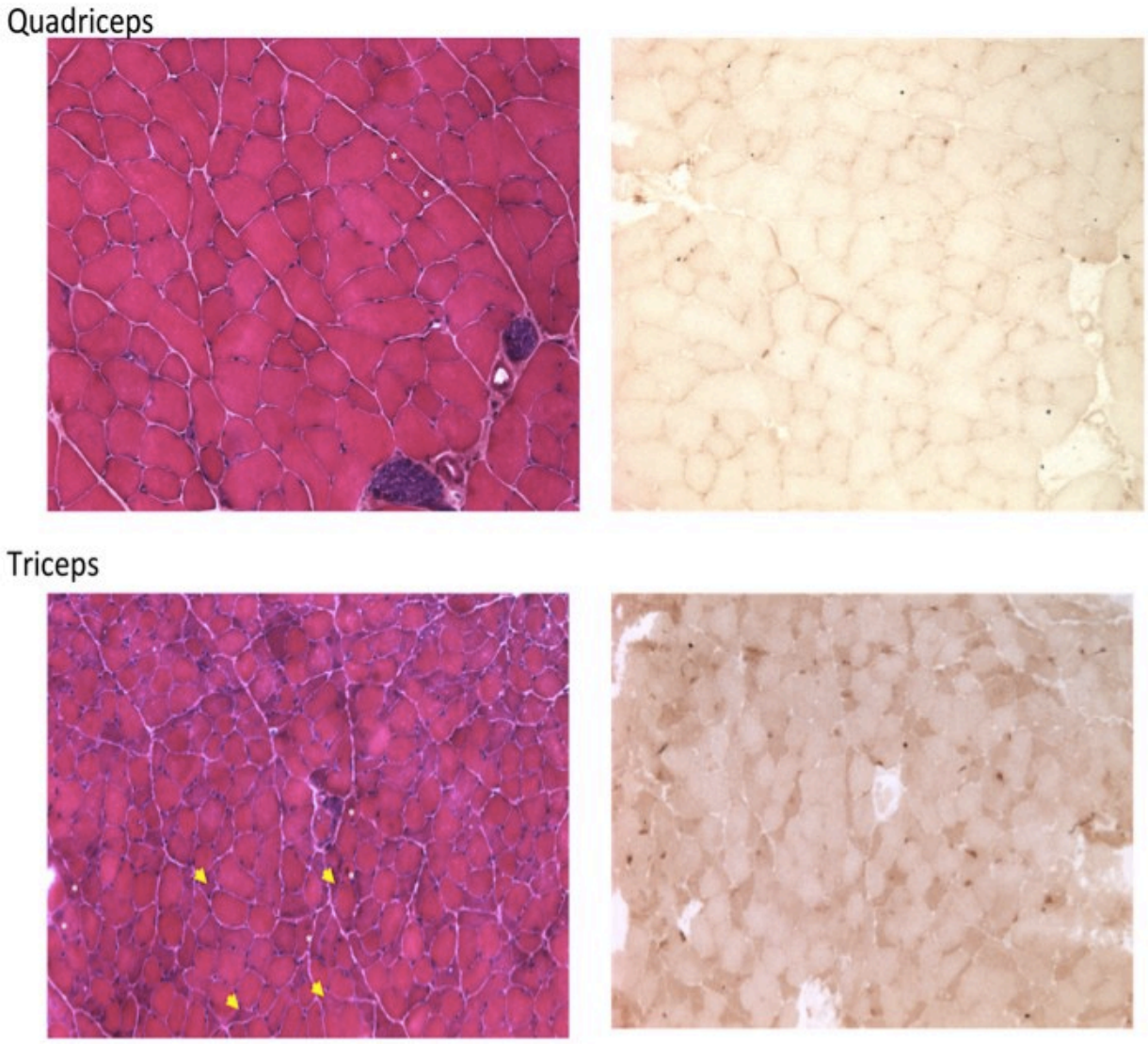

(D) H&E (left) staining of *Pitx1* transgenic (*TRE-Pitx1/mCK-tTA*) mouse treated with Vivo-morpholino showed obvious pathological improvement especially in quadriceps. H&E staining showed fewer angular fibers and fibers with central nuclei. Immunohistochemistry (right) showed less PITX1 positive nuclei compared with *Pitx1* transgenic (*TRE-Pitx1/mCK-tTA*) mouse treated with PBS.

3.3. Grip strength is improved after Vivo-morpholinos treatments in the *Pitx1* transgenic mice.

To determine whether Vivo-morpholinos and PMO treatments can improve muscle function, grip strength and rotarod were performed. Grip strength was tested on both forelimb and hindlimb once a day for five consecutive days after the fourth injection (Figure 7). For both forelimb and hindlimb, *Pitx1* transgenic mice treated with PBS (*TRE-Pitx1/mCK-tTA*) were significantly weaker than the control mice (*TRE-Pitx1* or *mCK-tTA*) (Figure 10A). *Pitx1* transgenic mice treated with Vivo-morpholinos were significantly stronger than those treated with PBS ($p< 0.05$). However, we did not observe significant improvement in grip strength in the mice treated with PMO.

Rotarod results varied among individual mice including the control mice (Figure 10B). Although not statistically significant, the *Pitx1* transgenic mice treated with Vivo-morpholinos performed better compared with mice treated with PBS or PMO and not significantly different from the control mice. *Pitx1* transgenic mice treated with PBS and PMO showed significantly lower performance than control mice as we previously reported.

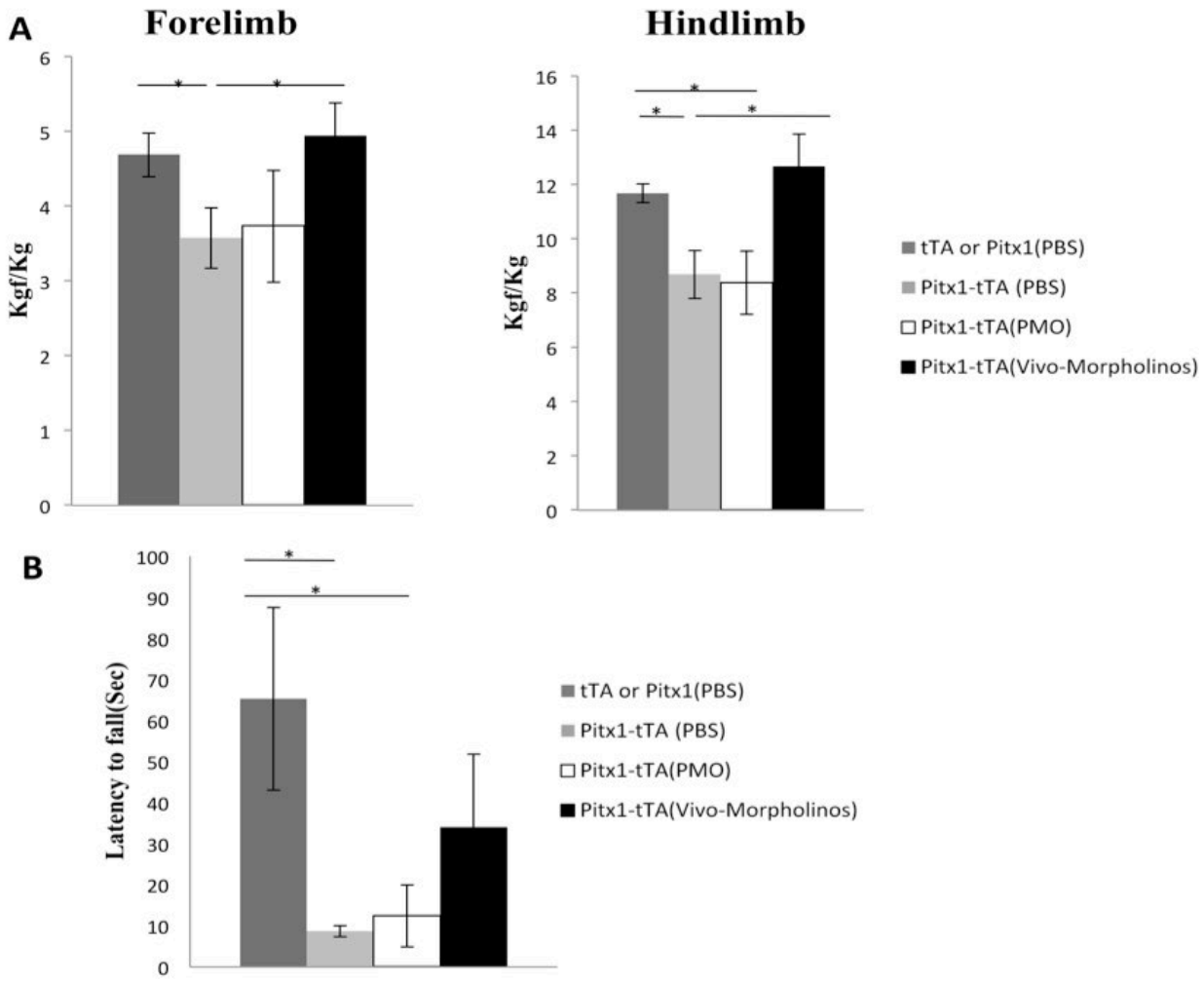

Figure 10. Muscle functional tests by grip strength (A) and rotarod (B) after fifth and sixth injections were applied respectively. One asterisk indicates significant differences with $p< 0.05$, and two asterisks indicate $p< 0.01$. (A) Grip strength measurement, both forelimb and hindlimb of *Pitx1* transgenic mice (*TRE-Pitx1/mCK-tTA*) treated with Vivo-morpholinos showed significantly better grip strength than the *Pitx1* transgenic mice treated with PBS. (B) Rotarod, *Pitx1* transgenic mice treated with Vivo-morpholinos stayed on rotarod three times longer than the *Pitx1* transgenic mice treated with PBS.

3.4. Muscle weight relative to body weight is improved in the *Pitx1* transgenic mice treated with Vivo-morpholinos.

The body weight of 12 transgenic (*TRE-Pitx1/mCK-tTA*) male mice and five control littermate male mice (*TRE-Pitx1* or *mCK-tTA*) were measured every two days, starting from the date that doxycycline was first removed from their water. Weekly body weight was plotted according to the treatment groups (Figure 11A). Previously we have shown that PITX1 over-expression lead to significant body weight and muscle weight loss as early as 5 weeks after gene induction (Pandey, Cabotage et al. 2012). We observed similar changes in this study; however the body weight change did not reach statistical significance. On the other hand, the body weight of the mice treated with Vivo-morpholinos was reduced significantly from week 4 on ($p< 0.05$).

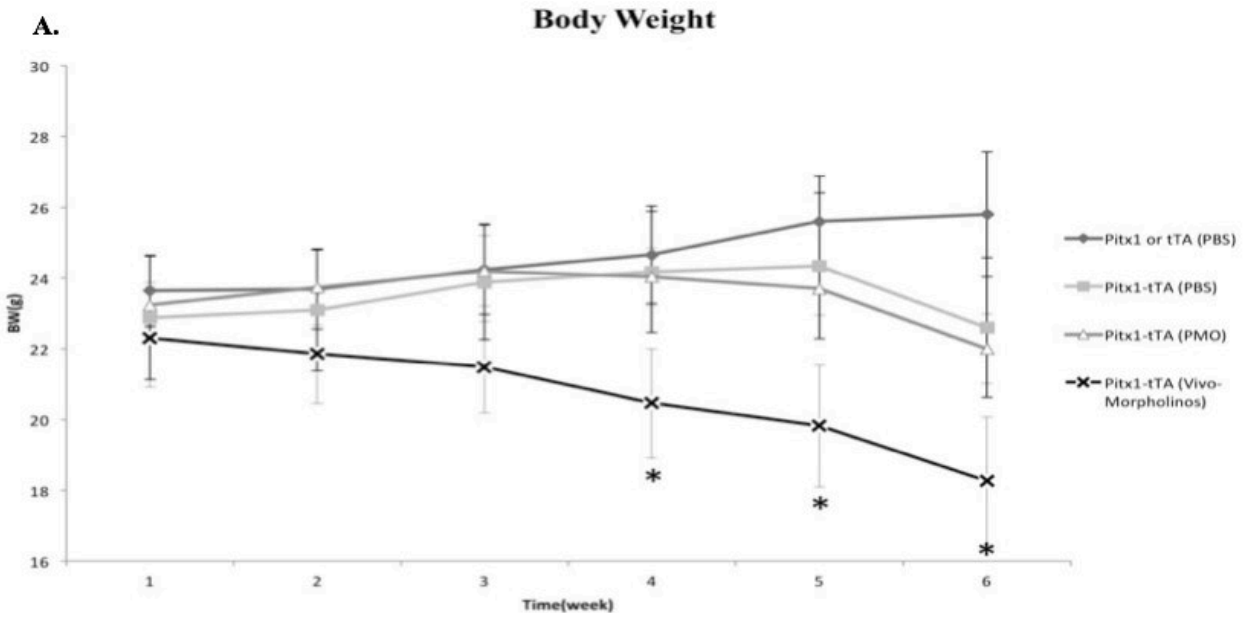

Figure 11A. The weekly body weight (gm, mean ± S.E.) after the first I.V. injection. One asterisk indicates significant differences with control mice (*TRE-Pitx1*or*mCK-tTA)* treated with PBS, $p< 0.05$, and two asterisks indicate $p< 0.01$. Starting from week four, the body weight of *Pitx1* transgenic mice (*TRE-Pitx1*/*mCK-tTA)* treated with Vivo-morpholinos was significant lower than control mice.

After being off doxycycline for six weeks, the mice were euthanized. Masseter, soleus, tibialis anterior, quadriceps, gastrocnemius, deltoid, triceps, biceps, diaphragm, from 12 *Pitx1* transgenic and five control mice were dissected and immediately weighed (Figure 11B). The result showed that PMO treatment didn't rescue the muscle weight. The muscle weight of both left and right collected muscle of the *Pitx1* transgenic mice treated with PMO was significantly lower than the control mice. In contrast, Vivo-morpholino treatment improved the muscle weight significantly while the body weight was reduced in these mice. The result suggests that the body weight loss seen in these mice is not a direct result of muscle weight loss.

B.

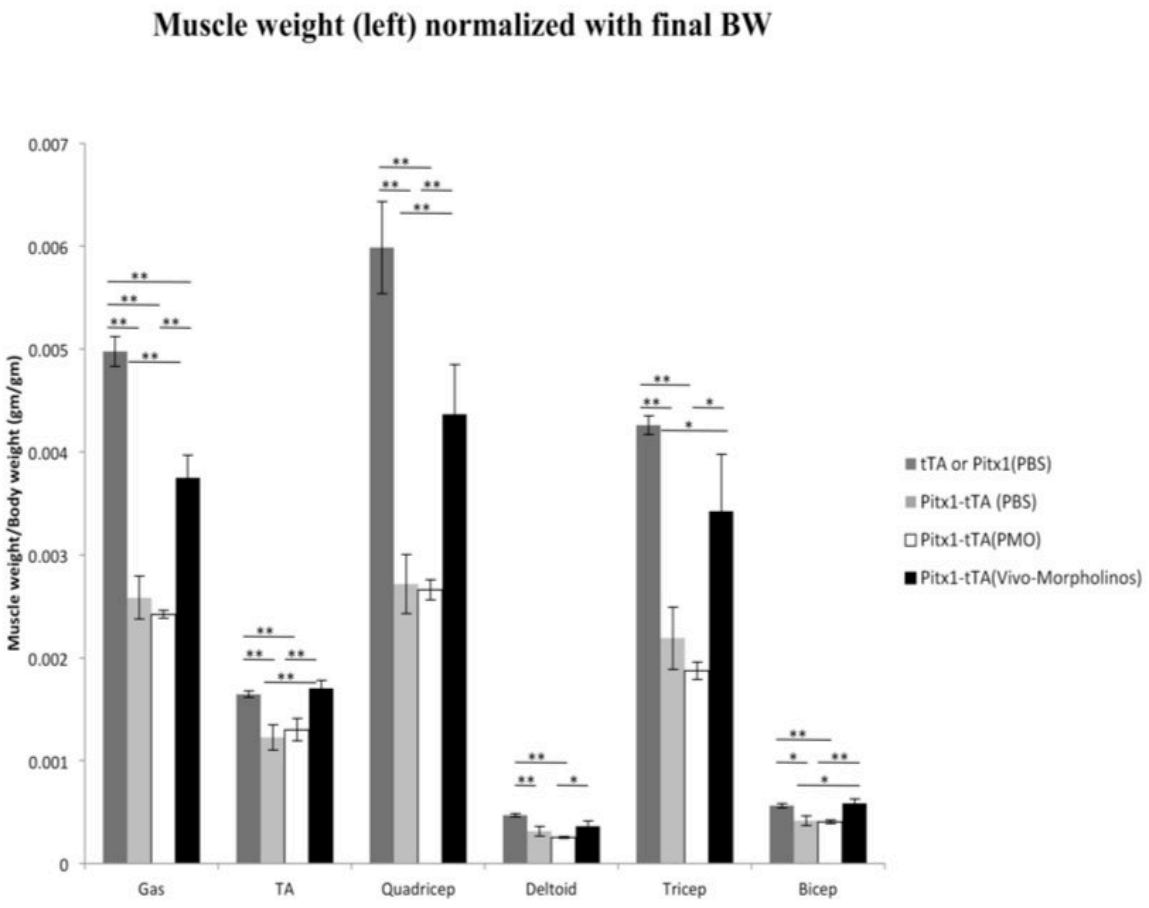

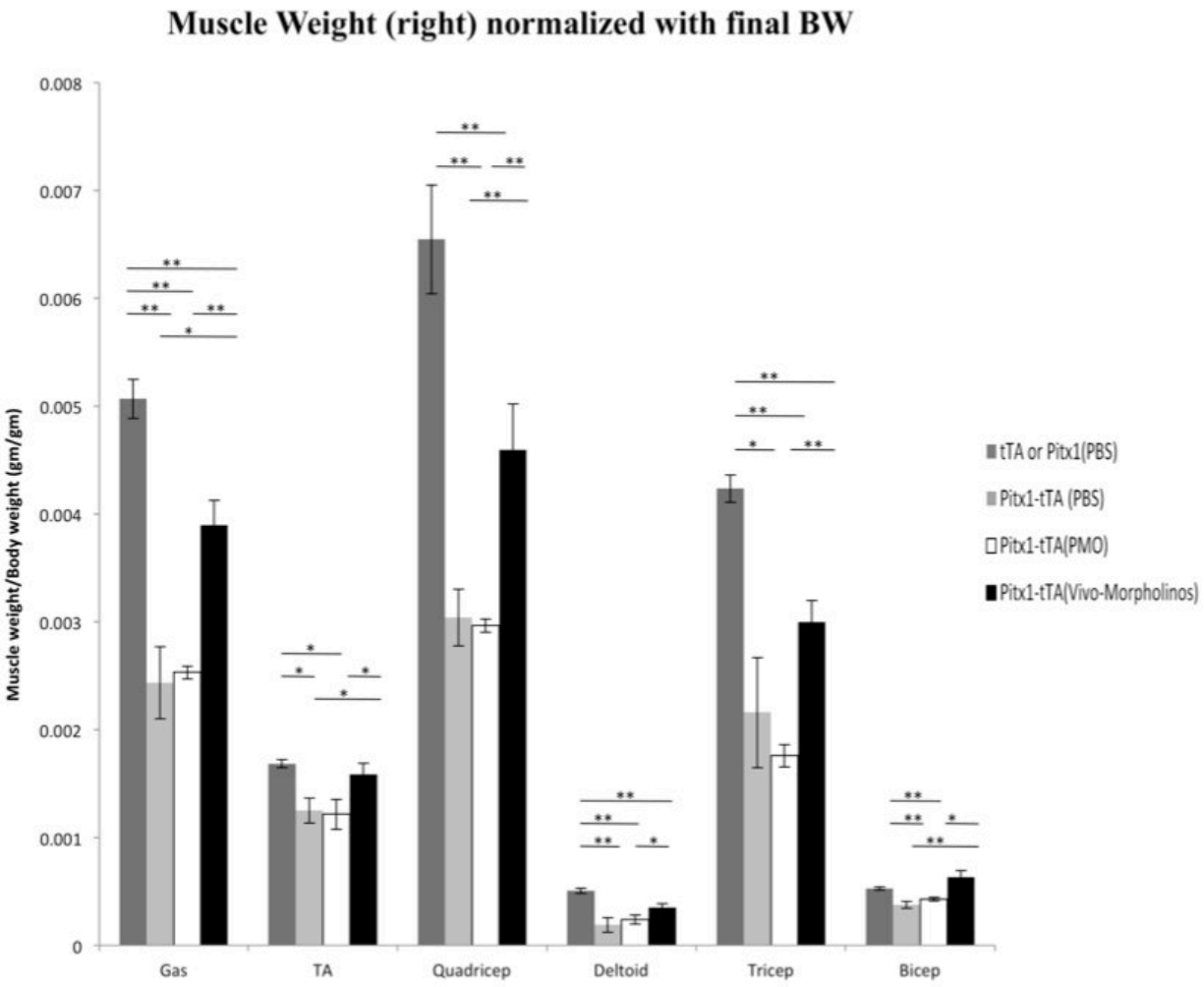

Figure 11B. Skeletal muscles weight normalized with body weight after sixth I.V. injections. One asterisk indicates significant differences with $p< 0.05$, and two asterisks indicate $p< 0.01$. In left gastrocnemius (Gas), tibialis anterior (TA), Quadriceps, Triceps and Bicep, the *Pitx1* transgenic mice treated with Vivo-morpholinos showed significant improvement compared with the *Pitx1* transgenic mice treated with PBS. In right Gas, TA, Quadriceps and Bicep, the *Pitx1* transgenic mice treated with Vivo-morpholinos showed significant improvement compared with the *Pitx1* transgenic mice treated with PBS.

3.5. Vivo-morpholinos treatments improved pathology in the *Pitx1* transgenic mice.

To examine the pathological improvement rather than the staining of PITX1 positive nuclei (as discussed in section 3.2.) of the *Pitx1* transgenic (*TRE-Pitx1/mCK-tTA*) mice treated with PMO and Vivo-morpholinos, triceps and quadriceps of all mice were frozen sectioned, and hematoxylin and eosin (H&E) staining was performed to visualize the pathological changes in the myofibers. The control mouse showed no angular-shaped atrophic fibers (Figure 9A). A large number of angular-shaped atrophic fibers and fibers with central nuclei were observed in muscle sections of the *Pitx1* transgenic mice treated with PBS (Figure 9B). Mice treated with PMO didn't show pathology improvement. The myofibers were small and a large amount of angular-shaped fibers and fibers with central nuclei were observed (Figure 9C). H&E staining of the mice treated with Vivo-morpholinos showed fewer angular-shaped atrophic fibers and fibers with central nuclei (Figure 9D). The results showed that Vivo-morpholinos treatment improved the muscle pathology but not PMO.

3.6. The fiber sizes of the mice treated with PBS, PMO and Vivo-morpholinos were not significantly different.

To measure the myofiber size of the mice treated with PMO and Vivo-morpholinos as an indication of pathological improvement, minimal Feret's diameter measurement (Briguet, Courdier-Fruh et al. 2004) on cross sections stained for laminin was performed (Figure 12A). Previous study showed that average fiber diameter size in the *Pitx1* transgenic mice was reduced by 41% in quadriceps (Pandey, Cabotage et al. 2012). In this study, we find that the average fiber diameter size in the quadriceps of the *Pitx1* transgenic (*TRE-Pitx1/mCK-tTA*) mice treated with PBS was reduced by 35 % of the control mice (*TRE-Pitx1*or *mCK-tTA*). The average fiber diameter size of the *Pitx1* transgenic mice treated with PMO and Vivo-morpholinos were

reduced by 30% and 33% respectively. Therefore, PMO and Vivo-morpholinos treatments didn't rescue the average fiber size significantly.

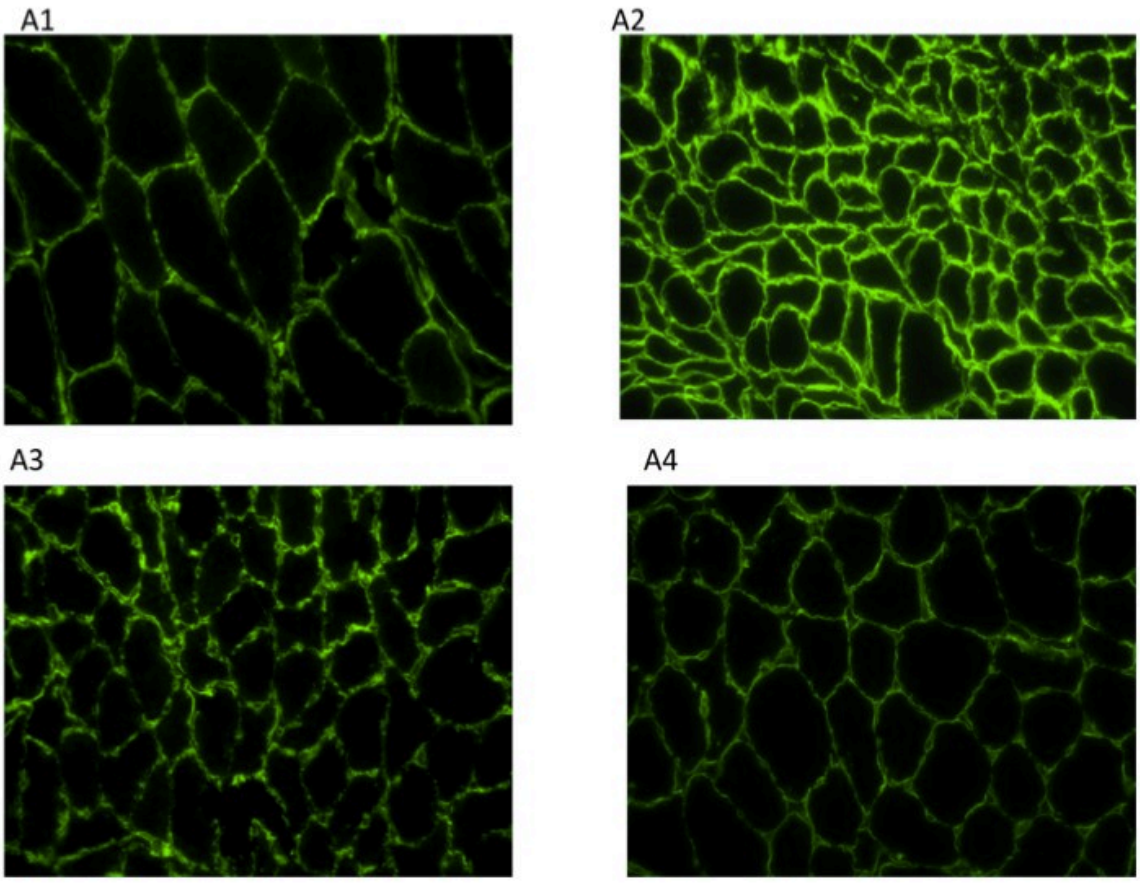

Figure 12A. Laminin staining of quadriceps of control mouse (*TRE-Pitx1*) (A1), *Pitx1* transgenic (*TRE-Pitx1/mCK-tTA*) mouse treated with PBS. (A2), *Pitx1* transgenic mouse injected with PMO (A3) and *Pitx1* transgenic mouse injected with Vivo-morpholinos (A4) for analyzing fiber size by measuring Feret's diameter using image J.

The myofibers then were ranked based on their size, and size was plotted size against the rank for each myofiber in order to assess the fiber size distribution using Kolmogorov–Smirnov test (Figure 12B). All fibers of the same treatment were plotted together to observe fiber size distribution of the control group, the *Pitx1* transgenic mice treated with PBS group, the *Pitx1* transgenic mice treated with PMO group and the group of *Pitx1* transgenic mice treated with Vivo-morpholinos. The result showed that smaller fibers of the mice treated with Vivo-morpholinos were slightly larger compared with the *Pitx1* transgenic mice treated with PBS. This finding suggests that the fiber size of the mice treated with Vivo-morpholinos was more homogenous than the mice treated with PBS, although the fiber size distribution of the *Pitx1* transgenic mice treated with PBS, PMO and Vivo-morpholinos didn't show a significant difference.

B.

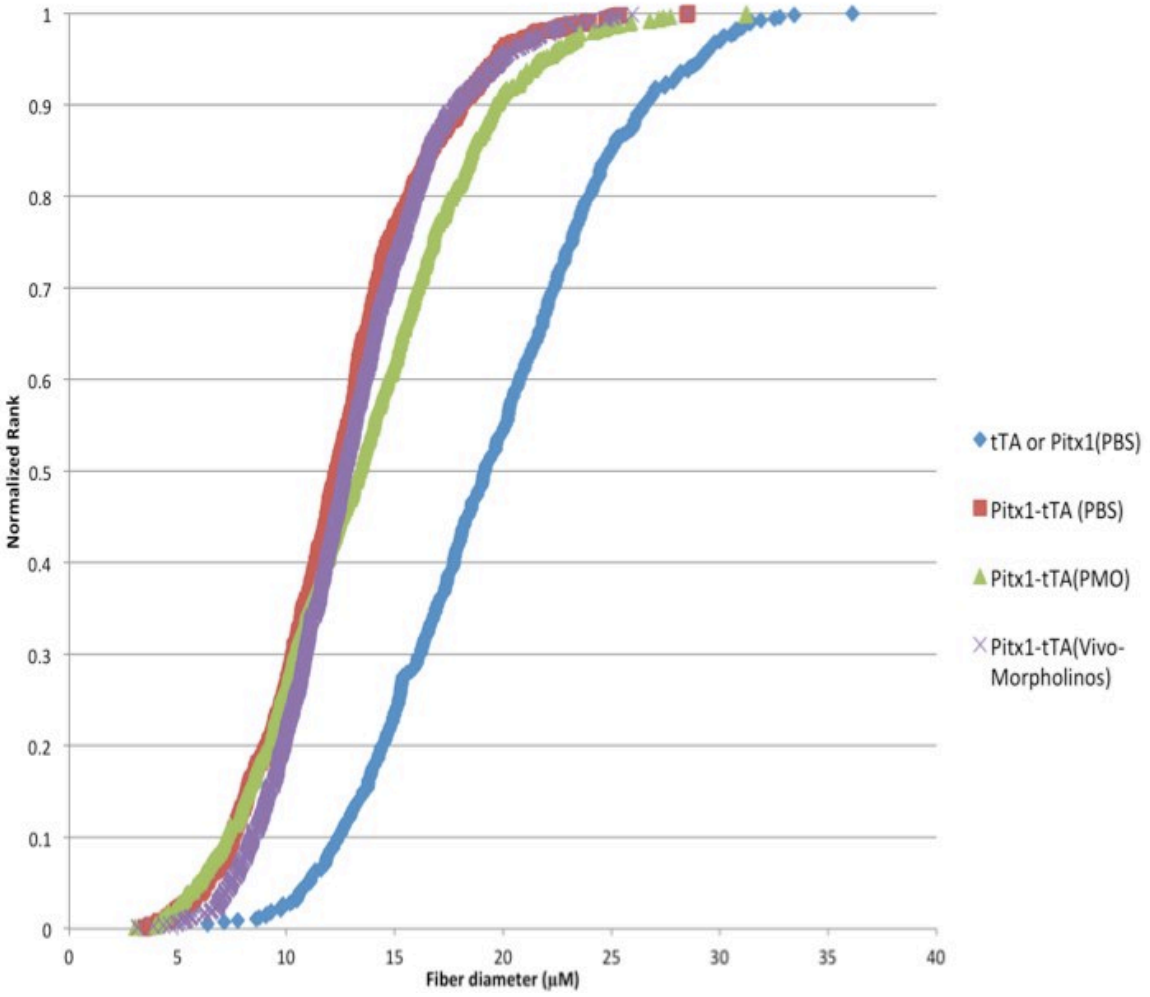

Figure 12B. **Fiber size distribution evaluation using minimal Feret's diameter measurement**. The normalized rank was plotted against fiber diameters of quadriceps. Fiber diameter of control mice (*mCK-tTA* or*TRE-Pitx1*) (blue), *Pitx1* transgenic (*TRE-Pitx1/mCK-tTA*) mice treated with PBS (Red), *Pitx1* transgenic mice injected with PMO (Green) and *Pitx1* transgenic mouse injected with Vivo-morpholinos (Purple) were plotted together. The result showed that both PMO and Vivo-morpholinos treatments didn't rescue the fiber size dramatically.

3.7. Angular fibers were significantly fewer after Vivo-morpholinos treatments.

In order to find a better indicator to evaluate the pathological improvement observed by H&E staining, the percentages of angular-shaped atrophic fibers were determined. Five random non-overlapping fields of H&E staining of quadriceps sections for each mouse were imaged and angular fibers were calculated blindly by the researcher. Control mice (*TRE-Pitx1* or *mCK-tTA*) have only 1% of angular fibers. Therefore, the percentage is significantly lower than all *Pitx1* transgenic mice (*TRE-Pitx1/mCK-tTA*). *Pitx1* transgenic mice treated with Vivo-morpholinos showed significantly lower percentage of angular fibers compared with PBS treated ones (Figure 13). The result suggested that Vivo-morpholinos treatments improved pathology of the *Pitx1* transgenic mice by reducing the percentage of angular fibers. On the other hand, mice treated with PMO still had many atrophy fibers.

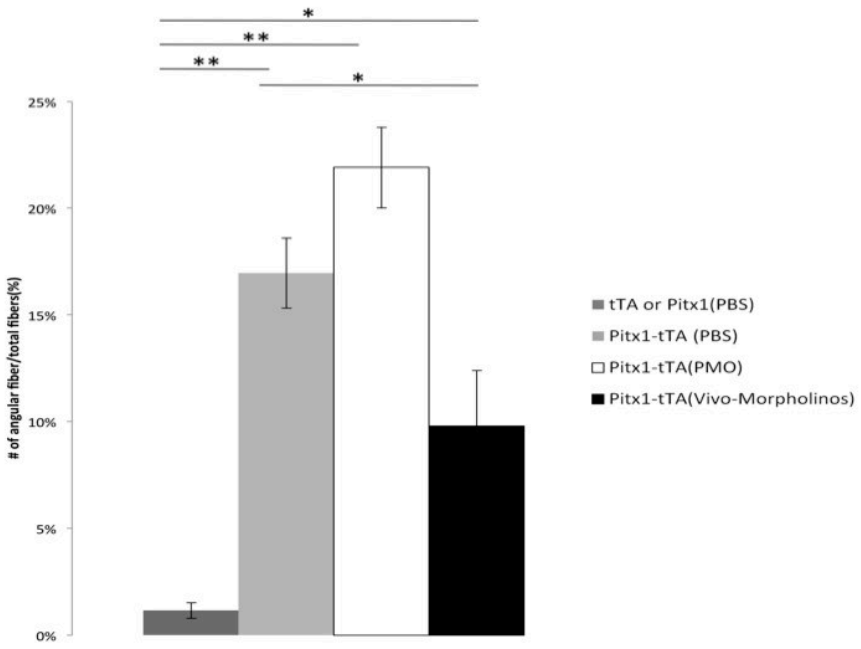

Figure 13. Percentage of angular fibers. The *Pitx1* transgenic mice (*TRE-Pitx1/mCK-tTA*) treated with Vivo-morpholinos have significantly lower percentage angular fibers than the *Pitx1* transgenic mice treated with PBS. One asterisk indicates significant differences with $p < 0.05$, and two asterisks indicate $p < 0.01$.

3.8. PITX1 expression and percentage of angular fibers is highly correlated.

To determine the correlation between PITX1 expression and angular fibers, the percentage of angular fibers was plotted against PITX1 expression level in quadriceps individually (Figure 14). Most of the *Pitx1* transgenic mice treated with PBS (Red) and PMO (Green) gathered at the upper right of the plot, which indicates that they had high PITX1 expression and high percentage of angular fibers, while mice treated with Vivo-morpholinos (Purple) had lower PITX1 expression and fewer angular fibers. PITX1 expression and percentage of angular fibers were highly correlated with the correlation coefficient of 0.84.

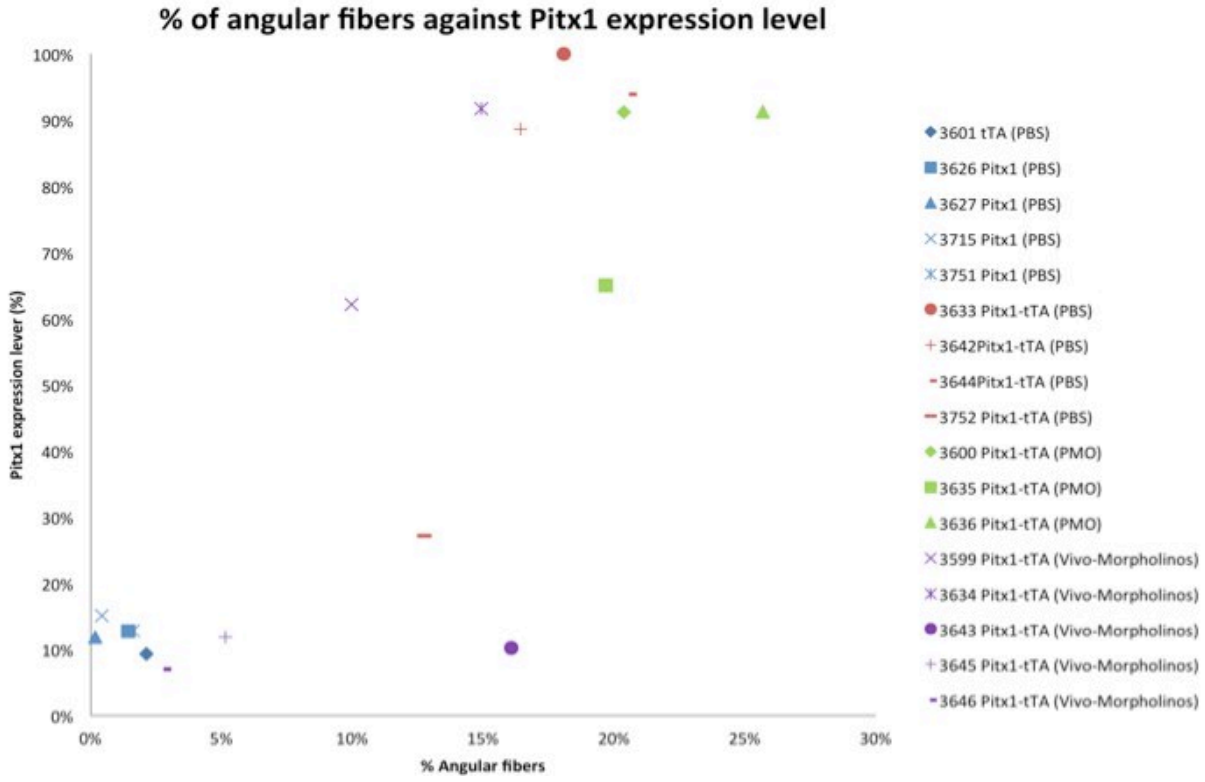

Figure 14. Correlation of angular fibers and PITX1 expression level. Most of the *Pitx1* transgenic treated with PBS (Red) and PMO (Green) mice gathered at the upper right of the plot, which indicates that they had high Pitx1 expression and high percentage of angular fibers. The correlation coefficient is 0.84.

3.9. Toxicity tests showed no obvious toxicity after Vivo-morpholinos treatments.

To test whether Vivo-morpholinos injections were toxic to mice, blood serum enzymes were examined (Figure 15). Alanine transaminase (ALT), Alkaline phosphatase (ALP), r-glutamyl transferase (GGT), and bilirubin are markers for liver toxicity. Blood urea nitrogen and creatine are indicators for kidney toxicity. Creatine kinase was tested for skeletal and heart muscle damage. Vivo-morpholinos injected mice did not have significant differences with both control mice (*mCK-tTA* or*TRE-Pitx1*) and the *Pitx1* transgenic mice treated with PBS. Therefore, there is no obvious toxicity detected in mice treated with Vivo-morpholinos mice.

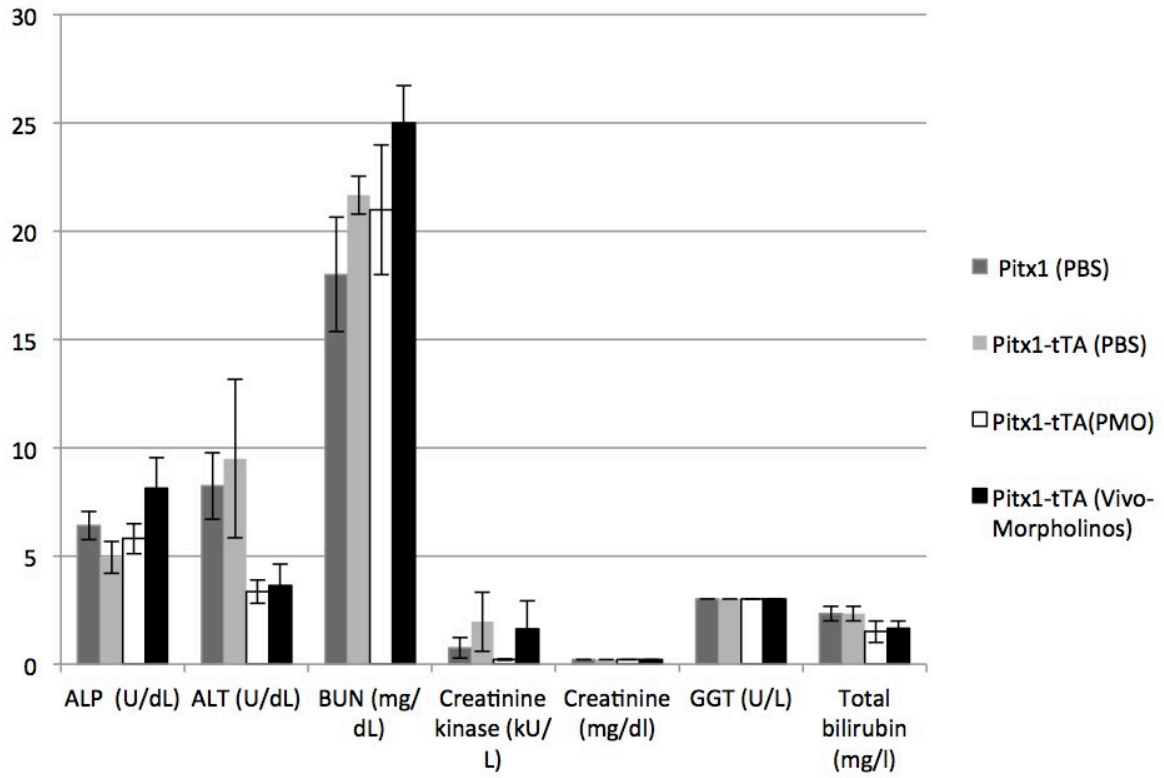

Figure 15. The levels of serum enzyme. Blood serum enzymes level of the mice treated with Vivo-morpholinos did not have significant differences between control and the *Pitx1* transgenic mice treated with PBS. The sample size of this experiment is three (n=3), which may increase the difficulties to acquire significant results.

4. Discussion

4.1. *In vivo* treatment for blocking protein translation

As discussed in the Introduction, the steric blocking mechanism of morpholinos has been shown to modify splicing of pre-mRNA, block the translation of mRNA or inhibit microRNA. Modifying splicing sites is commonly utilized to develop potential treatments for diseases. For example, PMO and PPMO have been studied for skipping exons in Duchenne Muscular Dystrophy (DMD). Both in mice and dog models, PMO and PPMO have been shown to restore dystrophin expression in high percentage of myofibers in order to generate a shorter but functional protein. Moreover, PPMO and Vivo-morpholinos have been shown to restore partial expression of dystrophin in cardiac muscles. PMO against exon 51 of dystrophin is currently in phase I clinical trial. Morpholinos have also been developed as treatments in other diseases such as β-thalassemia (Svasti, Suwanmanee et al. 2009) and restenosis (Kipshidze, Moses et al. 2001).

Moreover, PPMO also have been used for targeting virus. For instance, PPMO targeting the 5'terminal nucleotide or the 3' cyclization site of Dengue virus can decrease the viral titer in Vero cell (Stein, Huang et al. 2008). The same study also showed thatAG129 mice intraperitonealy injected with PPMO lived averaged eight days longer than untreated mice. Studies are also done at ebola Zaire virus VP24. PPMO targeting the translation site of VP24 transcripts had 100% protection of mice at 50μg per injection (Swenson, Warfield et al. 2009).

Using PMO to block the translation of specific mRNA is widely used to observe the function of the genes in developmental biology studies. However, not much work has been done by using this approach as therapeutic treatments. By translational blocking, PMO may benefit patients with diseases resulting from up-regulation of the disease causative genes. In this study,

we demonstrated the feasibility of using this strategy *in vivo*. We used the *Pitx1* transgenic mice model, which was developed to test the hypothesis that the over-expression of PITX1 in postnatal muscles may play a key role in the pathogenesis of FSHD. The *Pitx1* over-expressed mice showed that mice developed phenotypes of muscle weakness, myopathy, and the angular atrophic myofibers which was reported in FSHD previously. While it is not clear whether this model is a proper FSHD model, our study demonstrated the feasibility of knocking down a pathogenic protein *in vivo*. We showed Vivo-morpholinos successfully knocked down PITX1 in the *Pitx1* transgenic mice and improved the muscle function and pathology significantly.

PMO treatment in the *Pitx1* transgenic mice did not reduce PITX1 expression nor improve muscle function or pathology. PMO is not charged and has been shown difficult to be delivered into intact skeletal muscles (Moulton and Moulton 2008). The failure of delivering PMO into the *Pitx1* transgenic mice suggests that the mice do not have severe membrane damage as seen in the *mdx* mice and DMD. Therefore, PMO probably cannot be delivered into the muscle fibers to knock-down PITX1. Toxicity test result showed that the transgenic *Pitx1* mice treated with PBS didn't have high amount of creatine kinase in serum, which suggests that the muscles are not leaking out muscle-specific enzymes due to membrane damages (Figure 15). The result demonstrated that Vivo-morpholinos can be potential treatments for diseases overexpressing one or more unwanted genes in addition to FSHD.

4.2. Side effects observation of PMO, PPMO and Vivo-morpholinos

Research focusing on examining the toxicity of PMO has been done in both *mdx* mice and cynomolgus monkeys. In the study using *mdx* mice, PMO targeting dystrophin exon 51 (AVI-4658) and exon 23 (AVI-4225) were tested. Mice received intravenous injections once a

week for 12 weeks with the dose ranged from 12 to 960 mg/kg (Sazani 2011). The result showed that both AVI-4658 and AVI-4225 were well-tolerated even at the highest dose. An independent study in which *mdx* mice were treated with 1.5g/kg PMO for six months and showed no sign of toxicity (Wu, Xiao et al. 2011). In a studying monkeys received AVI-4658 weekly for 12 weeks with the highest dose of 320mg/kg (Sazani 2011). The result also demonstrated that AVI-4658 is tolerated well in monkeys. These results indicate that PMO could be used safely as drugs for long-term systemic treatment of DMD.

Several studies examined the toxicity of PPMO and Vivo-morpholinos, which are the same morpholinos with either peptides or octaguanidinium modification to improve delivery into cells. In one study, PPMO which targets human exon 50 (AVI-5038) were injected into the cynomolgus monkey weekly with 9mg/kg per injection for four weeks. The study showed that monkeys received the PPMO injections had kidney mild tubular degeneration (Moulton and Moulton 2008). However, the toxicity of PPMO was not observed in *mdx* mice even in a much higher dose (30mg/kg biweekly for three months) (Wu, Moulton et al. 2008). Therefore, these results suggest that different species may respond to PPMO differently. Although the causes of toxicity are not known, one of the possibilities is that the cationic property of PPMO causes off-target effects. The most essential factor making PMO free from off target effects is because of their non-ionic backbones. However, with the arginine-rich cell penetrating peptides, the morpholinos with positive charge may interact with other proteins and molecules and result in off-target effect. One study has shown that the degradation of the conjugated peptides was found in some tissues (Lebleu, Moulton et al. 2008). It is possible that the residues after digestion may interact with other molecules and result in off target effect.

To minimize the problems caused by the peptide-conjugated Morpholinos, Vivo-morpholinos was used in this study. The toxicity of PMO and Vivo-morpholinos injections was tested by measuring the activity of blood serum enzymes. We didn't see any sign of liver and kidney of toxicity from the blood serum enzyme tests (Figure 15). However, more detailed toxicity tests need to be investigated such as microscopic evaluation of other organs.

Previous studies have shown that the body weight of *mdx* mice receiving 10 weeks of Vivo-morpholinos I.V. injections (6mg/kg) remained similar to control mice and no obvious toxicity was found (Wu, Li et al. 2009). On the other hand, in this study, the *Pitx1* transgenic mice which received Vivo-morpholinos showed significant body weight loss after the fourth Vivo-morpholinos injection (Figure 11A). However, the muscle weight relative to body weight and muscle strength improved in the *Pitx1* transgenic mice treated with Vivo-morpholinos. The result implied that the body weight loss is not due to muscle loss. Considering no toxicity was observed, the effect of Vivo-morpholinos can be affecting metabolism of the mice.

One of the possibilities which may result in body weight loss is the loss of appetite. Pituitary gland releases hormones which control appetite. It is believed that *Pitx1* can independently activate and synergize with PIT-1 on pituitary-specific target gene promoters, which may affect the development of pituitary gland (Szeto, Ryan et al. 1996). Is it possible that pituitary gland development was affected by knocking down PITX1, which in turn affected the release of hormones associated with appetite? There are two reasons why we don't think Vivo-morpholinos treatments affected pituitary gland in this study. First, although *PITX1* may affect the development of pituitary gland, the experiment was started until mice had reached the age of eight weeks. Therefore, theoretically pituitary gland should have been fully developed at the start of the experiment. Second, research has shown that Vivo-morpholino can't be delivered to

the brain by intravenous injections (Morcos, P. A., 2008, Biotechniques). As a result, Vivo-morpholinos should not affect PITX1 expression in brain. The cause of the body weight loss is not clear with the data in hand and needs to be investigated further.

5. Reference

Abes, R., H. M. Moulton, et al. (2008). "Delivery of steric block morpholino oligomers by (R-X-R)4 peptides: structure-activity studies." Nucleic Acids Res**36**(20): 6343-54.

Bosnakovski, D., R. S. Daughters, et al. (2009). "Biphasic myopathic phenotype of mouse DUX, an ORF within conserved FSHD-related repeats." PLoS One**4**(9): e7003.

Bosnakovski, D., Z. Xu, et al. (2008). "An isogenetic myoblast expression screen identifies DUX4-mediated FSHD-associated molecular pathologies." Embo J**27**(20): 2766-79.

Briguet, A., I. Courdier-Fruh, et al. (2004). "Histological parameters for the quantitative assessment of muscular dystrophy in the mdx-mouse." Neuromuscul Disord**14**(10): 675-82.

Calvisi, D. F., S. Ladu, et al. (2011). "Inactivation of Ras GTPase-activating proteins promotes unrestrained activity of wild-type Ras in human liver cancer." J Hepatol**54**(2): 311-9.

Carroll, J. E. (1979). "Facioscapulohumeral and scapuloperoneal syndromes." Handbook of Clinical Neurology**40**: 415-431.

Civas, A., M. L. Island, et al. (2002). "Regulation of virus-induced interferon-A genes." Biochimie**84**(7): 643-54.

Dixit, M., E. Ansseau, et al. (2007). "DUX4, a candidate gene of facioscapulohumeral muscular dystrophy, encodes a transcriptional activator of PITX1." Proc Natl Acad Sci U S A**104**(46): 18157-62.

Fitzsimons, R. B., E. B. Gurwin, et al. (1987). "Retinal vascular abnormalities in facioscapulohumeral muscular dystrophy. A general association with genetic and therapeutic implications." Brain**110 (Pt 3)**: 631-48.

Gabellini, D., G. D'Antona, et al. (2006). "Facioscapulohumeral muscular dystrophy in mice overexpressing FRG1." Nature**439**(7079): 973-7.

Gabellini, D., M. R. Green, et al. (2002). "Inappropriate gene activation in FSHD: a repressor complex binds a chromosomal repeat deleted in dystrophic muscle." Cell**110**(3): 339-48.

Gabriels J, B. M., Ding H, De Vriese A, Plaisance S, van der Maarel SM, Padberg GW, Frants RR, Hewitt JE, Collen D, et al. (1999). "Nucleotide sequence of the partially deleted D4Z4 locus in a patient with FSHD identifies a putative gene within each 3.3 kb element." Gene**236(1)**(1): 25-32.

Ghersa, P., R. P. Gobert, et al. (1998). "Highly controlled gene expression using combinations of a tissue-specific promoter, recombinant adenovirus and a tetracycline-regulatable transcription factor." Gene Ther**5**(9): 1213-20.

Gurnett, C. A., F. Alaee, et al. (2008). "Asymmetric lower-limb malformations in individuals with homeobox PITX1 gene mutation." Am J Hum Genet**83**(5): 616-22.

Hudziak, R. M., E. Barofsky, et al. (1996). "Resistance of morpholino phosphorodiamidate oligomers to enzymatic degradation." Antisense Nucleic Acid Drug Dev**6**(4): 267-72.

Jiang, G., F. Yang, et al. (2003). "Testing the position-effect variegation hypothesis for facioscapulohumeral muscular dystrophy by analysis of histone modification and gene expression in subtelomeric 4q." Hum Mol Genet**12**(22): 2909-21.

Kang, H., P. J. Chou, et al. (1992). "Stacking interactions of ApA analogues with modified backbones." Biopolymers**32**(10): 1351-63.

Kawasaki, H. and K. Taira (2004). "Induction of DNA methylation and gene silencing by short interfering RNAs in human cells." Nature**431**(7005): 211-7.

Kipshidze, N., J. Moses, et al. (2001). "Perspectives on antisense therapy for the prevention of restenosis." Curr Opin Mol Ther**3**(3): 265-77.

Kloosterman, W. P., A. K. Lagendijk, et al. (2007). "Targeted inhibition of miRNA maturation with morpholinos reveals a role for miR-375 in pancreatic islet development." PLoS Biol**5**(8): e203.

Kolfschoten, I. G., B. van Leeuwen, et al. (2005). "A genetic screen identifies PITX1 as a suppressor of RAS activity and tumorigenicity." Cell**121**(6): 849-58.

Kowaljow, V., A. Marcowycz, et al. (2007). "The DUX4 gene at the FSHD1A locus encodes a pro-apoptotic protein." Neuromuscul Disord**17**(8): 611-23.

Krieg, A. M., A. K. Yi, et al. (1995). "CpG motifs in bacterial DNA trigger direct B-cell activation." Nature**374**(6522): 546-9.

Lamonerie, T., J. J. Tremblay, et al. (1996). "Ptx1, a bicoid-related homeo box transcription factor involved in transcription of the pro-opiomelanocortin gene." Genes Dev**10**(10): 1284-95.

Lanctot, C., A. Moreau, et al. (1999). "Hindlimb patterning and mandible development require the Ptx1 gene." Development**126**(9): 1805-10.

Lebleu, B., H. M. Moulton, et al. (2008). "Cell penetrating peptide conjugates of steric block oligonucleotides." Adv Drug Deliv Rev**60**(4-5): 517-29.

Lin, M. Y. and I. Nonaka (1991). "Facioscapulohumeral muscular dystrophy: muscle fiber type analysis with particular reference to small angular fibers." Brain Dev**13**(5): 331-8.

Liu, D. X. and P. E. Lobie (2007). "Transcriptional activation of p53 by Pitx1." Cell Death Differ**14**(11): 1893-907.

Logan, M. and C. J. Tabin (1999). "Role of Pitx1 upstream of Tbx4 in specification of hindlimb identity." Science**283**(5408): 1736-9.

Marcil, A., E. Dumontier, et al. (2003). "Pitx1 and Pitx2 are required for development of hindlimb buds." Development**130**(1): 45-55.

Masny, P. S., U. Bengtsson, et al. (2004). "Localization of 4q35.2 to the nuclear periphery: is FSHD a nuclear envelope disease?" Hum Mol Genet**13**(17): 1857-71.

Morcos, P. A., Y. Li, et al. (2008). "Vivo-Morpholinos: a non-peptide transporter delivers Morpholinos into a wide array of mouse tissues." Biotechniques**45**(6): 613-4, 616, 618 passim.

Moulton, H. M. and J. D. Moulton (2008). "Morpholinos and their peptide conjugates: therapeutic promise and challenge for Duchenne muscular dystrophy." Biochim Biophys Acta**1798**(12): 2296-303.

Moulton, J. D. and S. Jiang (2009). "Gene knockdowns in adult animals: PPMOs and vivo-morpholinos." Molecules**14**(3): 1304-23.

Padberg, G. (1982). Facioscapulohumeral disease. Thesis. Leiden, The Netherlands: University of Leiden.

Padberg, G. W., O. F. Brouwer, et al. (1995). "On the significance of retinal vascular disease and hearing loss in facioscapulohumeral muscular dystrophy." Muscle Nerve**2**: S73-80.

Pandey, S. N., J. Cabotage, et al. (2012). "Conditional over-expression of PITX1 causes sketetal muscle dystrophy in mice." Biology open.

Rothbard, J. B., T. C. Jessop, et al. (2004). "Role of membrane potential and hydrogen bonding in the mechanism of translocation of guanidinium-rich peptides into cells." J Am Chem Soc**126**(31): 9506-7.

Sazani, P., Van Ness, K. P., Weller, D. L., Poage, D., Nelson, K., and Shrewsbury S. B. (2011). "Chemical and Mechanistic Toxicology Evaluation of Exon Skipping

Phosphorodiamidate Morpholino Oligomers in mdx mice." International Journal of Toxicology**30**(3): 322-333.

Sazani, P., Van Ness, K. P., Weller, D. L., Poage, D., Nelson, K., and Shrewsbury S. B. (2011). "Repeat-Dose Toxicology Evaluation in Cynomolgus Monkeys of AVI-4658, a Phosphorodiamidate Morpholino Oligomer (PMO) Drug for the Treatment of Duchenne Muscular Dystrophy." International Journal of Toxicology**30**(3): 313-321.

Sledz, C. A., M. Holko, et al. (2003). "Activation of the interferon system by short-interfering RNAs." Nat Cell Biol**5**(9): 834-9.

Stein, C. A. K., A. (1984). "Non-antisense effects of oligodeoxynucleotides." Antisense Technology a Practical Approach: pp. 241-264.

Stein, D. A., C. Y. Huang, et al. (2008). "Treatment of AG129 mice with antisense morpholino oligomers increases survival time following challenge with dengue 2 virus." J Antimicrob Chemother**62**(3): 555-65.

Summerton, J. (1999). "Morpholino antisense oligomers: the case for an RNase H-independent structural type." Biochim Biophys Acta**1489**(1): 141-58.

Summerton, J. (2005). "Morpholino Antisense Oligos: Applications in Biopharmaceutical Research." Innovations in Pharmaceutical Technology (17).

Summerton, J. and D. Weller (1997). "Morpholino antisense oligomers: design, preparation, and properties." Antisense Nucleic Acid Drug Dev**7**(3): 187-95.

Summerton, J. E. (2007). "Morpholino, siRNA, and S-DNA compared: impact of structure and mechanism of action on off-target effects and sequence specificity." Curr Top Med Chem**7**(7): 651-60.

Svasti, S., T. Suwanmanee, et al. (2009). "RNA repair restores hemoglobin expression in IVS2-654 thalassemic mice." Proc Natl Acad Sci U S A**106**(4): 1205-10.

Swenson, D. L., K. L. Warfield, et al. (2009). "Chemical modifications of antisense morpholino oligomers enhance their efficacy against Ebola virus infection." Antimicrob Agents Chemother**53**(5): 2089-99.

Szeto, D. P., C. Rodriguez-Esteban, et al. (1999). "Role of the Bicoid-related homeodomain factor Pitx1 in specifying hindlimb morphogenesis and pituitary development." Genes Dev**13**(4): 484-94.

Szeto, D. P., A. K. Ryan, et al. (1996). "P-OTX: a PIT-1-interacting homeodomain factor expressed during anterior pituitary gland development." Proc Natl Acad Sci U S A**93**(15): 7706-10.

Tawil, R. (2008). "Facioscapulohumeral Muscular Dystrophy." Neorotherapeutics**5**: 601-606.

Tremblay, J. J., C. Lanctot, et al. (1998). "The pan-pituitary activator of transcription, Ptx1 (pituitary homeobox 1), acts in synergy with SF-1 and Pit1 and is an upstream regulator of the Lim-homeodomain gene Lim3/Lhx3." Mol Endocrinol**12**(3): 428-41.

Tyler, F. H., Stephens, F. E, (1949). "Studies in Disorders of Muscle II Clinical Manifestations and Inheritance of Facioscapulohumeral Dystrophy in a Large Family." 640-660.

van Deutekom, J. C., C. Wijmenga, et al. (1993). "FSHD associated DNA rearrangements are due to deletions of integral copies of a 3.2 kb tandemly repeated unit." Hum Mol Genet**2**(12): 2037-42.

van Overveld, P. G., R. J. Lemmers, et al. (2003). "Hypomethylation of D4Z4 in 4q-linked and non-4q-linked facioscapulohumeral muscular dystrophy." Nat Genet**35**(4): 315-7.

Wegel, E. and P. Shaw (2005). "Gene activation and deactivation related changes in the three-dimensional structure of chromatin." Chromosoma**114**(5): 331-7.

Wender, P. A., D. J. Mitchell, et al. (2000). "The design, synthesis, and evaluation of molecules that enable or enhance cellular uptake: peptoid molecular transporters." Proc Natl Acad Sci U S A**97**(24): 13003-8.

Wu, B., Y. Li, et al. (2009). "Octa-guanidine morpholino restores dystrophin expression in cardiac and skeletal muscles and ameliorates pathology in dystrophic mdx mice." Mol Ther**17**(5): 864-71.

Wu, B., H. M. Moulton, et al. (2008). "Effective rescue of dystrophin improves cardiac function in dystrophin-deficient mice by a modified morpholino oligomer." Proc Natl Acad Sci U S A**105**(39): 14814-9.

Wu, B., B. Xiao, et al. (2011). "One-year treatment of morpholino antisense oligomer improves skeletal and cardiac muscle functions in dystrophic mdx mice." Mol Ther**19**(3): 576-83.

Yaswen, P., M. R. Stampfer, et al. (1993). "Effects of sequence of thioated oligonucleotides on cultured human mammary epithelial cells." Antisense Res Dev**3**(1): 67-77.

Zeng, W., J. C. de Greef, et al. (2009). "Specific loss of histone H3 lysine 9 trimethylation and HP1gamma/cohesin binding at D4Z4 repeats is associated with facioscapulohumeral dystrophy (FSHD)." PLoS Genet**5**(7): e1000559.